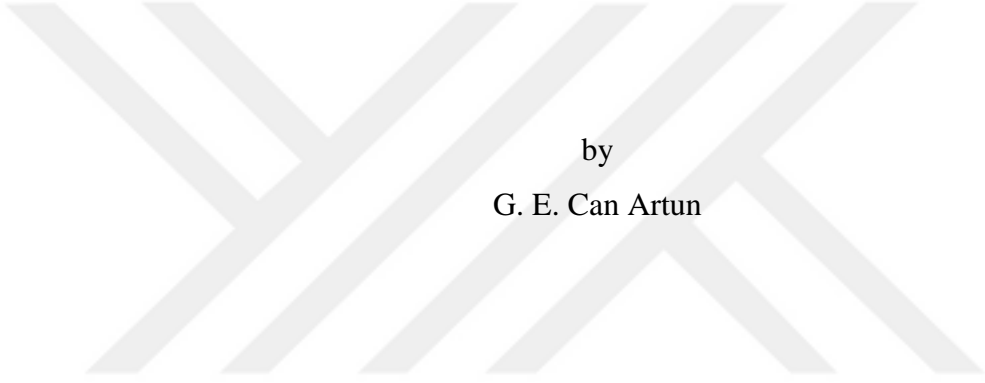


NONLINEAR DYNAMICS AND POSSIBLE CHAOTICITY IN CONDENSED
MATTER SYSTEMS



by
G. E. Can Artun

Submitted to Graduate School of Natural and Applied Sciences
in Partial Fulfillment of the Requirements
for the Degree of Master of Science in
Physics

Yeditepe University
2015

NONLINEAR DYNAMICS AND POSSIBLE CHAOTICITY IN CONDENSED
MATTER SYSTEMS

APPROVED BY:

Prof. Avadis S. Hacınılyan
(Thesis Supervisor)

.....

Assoc. Prof. Ş. İpek Karaaslan

.....

Assist. Prof. H. Ahmet Yıldırım

.....

DATE OF APPROVAL:/...../2015

ACKNOWLEDGEMENTS

I would like to thank especially my thesis adviser Prof. Avadis Hacınliyan for his inexhaustible patience and support. I also owe special thanks to my parents who gave the motivation and support that I needed.



ABSTRACT

NONLINEAR DYNAMICS AND POSSIBLE CHAOTICITY IN CONDENSED MATTER SYSTEMS

Possible chaotic behavior in the transient current through a sample of $\text{As}_2\text{S}_3(\text{Ag})$ and $\text{As}_2\text{Se}_3(\text{Al})$ thin films was examined with time series analysis, rescaled range (R/S) analysis and q -Gaussian analysis. R/S analysis shows that there are two regimes of fractal behavior; one seems like because of short time scale relaxation and the other one seems like because of long term chaotic behavior. The mutual information data indicate the necessity of noise reduction using a moving average. Extending the moving average window gives correspondingly large delay times as expected. The indicated delay time starts at 20s and grows up to 250s. The false nearest neighbor results also indicate a value around 10. A robust increase in the Lyapunov exponent stretching graphs confirms long term chaos; the result is not sensitive to the precise values of the delay time and embedding dimension. In the q -Gaussian analysis, the fitted long tailed and peaked q -Gaussian curves are completely different from a normal Gaussian. q values greater than one show that the results are consistent with the chaos analysis results.

ÖZET

DOĞRUSAL OLMAYAN DEVİMBİLİM VE YOĞUN ÖZDEK DİZGELERİNDE OLASI KAOSALLIK

$As_2S_3(Ag)$ ile $As_2Se_3(Al)$ ince film örneklerinden geçen geçici akımlardaki olası kaossal davranış zaman serileri çözümlemesi, yeniden-boyutlandırılmış aralık (R/S) çözümlemesi ve q -Gaussyan (q -Gaussian) çözümlemesi ile incelenmiştir. R/S çözümlemesi iki fraktal düzenin olduğunu göstermiştir; biri kısa erimli gevşemeden, diğeri de uzun erimli kaossal davranıştan ileri geliyor gibi görünmektedir. Ortak bilgi verileri, hareketli ortalamayla gürültü azaltmaya gereksinimi göstermektedir. Belirtilen gecikme zamanları 20sn'de başlayıp 250sn'ye kadar ilerlemektedir. Yanlış en yakın komşu incelemesi de 10 civarını göstermektedir. Lyapunov üstellerindeki sert yükseliş uzun erimli kaosu işaret etmekte olup sonuçlar gecikme zamanlarına ve gömülü boyuta hassas değildir. q -Gaussyan çözümlemesinde uydurulmuş q -Gaussyan eğrileri uzun kuyruklarıyla ve sivri tepeleriyle olağan Gaussyan eğrisinden oldukça farklı olarak elde edildi. Birden büyük q katsayı değerleri bu son sonuçların ilk elde edilen sonuçlarla tutarlı olduklarını göstermektedir.

TABLE OF CONTENTS

ACKNOWLEDGEMENTS.....	iii
ABSTRACT.....	iv
ÖZET	v
LIST OF FIGURES	ix
LIST OF TABLES.....	xii
LIST OF SYMBOLS/ABBREVIATIONS.....	xiii
1. INTRODUCTION.....	1
2. NONLINEAR DYNAMICAL SYSTEMS	3
2.1. A BRIEF HISTORY OF DYNAMICS.....	3
2.2. REPRESENTATION OF DYNAMICAL SYSTEMS	4
2.2.1. Linearization: A Tool to analyze the behaviors.....	7
2.3. PHASE PLANE AND VECTOR FIELDS	8
2.4. LIMIT CYCLES	11
2.5. ATTRACTORS I: LORENZ SYSTEM.....	13
2.5.1. Lorenz Equations	13
2.6. ATTRACTORS II: STRANGE ATTRACTORS.....	17
2.6.1. Lorenz Attractor.....	17
2.6.2. Sensitive Dependence on Initial Conditions and Chaos	19
2.6.2.1. Lyapunov Exponent.....	20
2.6.2.2. Smale's Horseshoe.....	21
2.6.2.3. Chaos.....	22
2.7. DISCRETE-TIME DYNAMICAL SYSTEM.....	22
2.7.1. Poincaré Maps.....	23
2.7.1.1. Stability of Periodic Orbits.....	24
2.7.2. Lyapunov Exponent for 1-D Maps	27
2.8. THE LOGISTIC MAP	28
2.9. BIFURCATIONS.....	31
2.9.1. Period Doubling and Saddle-Node Bifurcations.....	31
2.9.2. Transcritical Bifurcation.....	35

2.9.3. Pitchfork Bifurcation.....	36
2.10. FRACTALS.....	37
2.10.1. Dimension	39
2.10.2. Cantor Set.....	40
2.10.3. Chaos Game.....	41
3. DIFFUSION IN CONDENSED MATTER.....	44
3.1. FICK'S LAWS OF DIFFUSION.....	44
3.2. COLLISION MODEL AND BROWNIAN DIFFUSION.....	45
3.3. ANOMALOUS DIFFUSION.....	46
4. NONEXTENSIVESTATISTICALMECHANICS.....	48
4.1. BOLTZMANN-GIBBS STATISTICAL MECHANICS.....	48
4.2. GENERALIZATION OF THE BOLTZMANN-GIBBS STATISTICAL MECHANICS.....	50
4.3. GENERALIZED DISTRIBUTIONS AND THE q -GAUSSIAN.....	52
5. ANALYSIS OF CHAOTIC SYSTEM BEHAVIORS.....	55
5.1. PHASE SPACE RECONSTRUCTION.....	56
5.2. CHOOSING TIME DELAYS.....	57
5.2.1. Auto-correlation Function.....	57
5.2.2. Mutual Information.....	58
5.3. CHOOSING THE DIMENSION.....	59
5.3.1. False Nearest Neighborhood Method	59
5.4. FINDING THE LYAPUNOV EXPONENT.....	61
5.5. HURST'S RESCALED RANGE ANALYSIS.....	61
6. CHAOS IN CONDENSED MATTER SYSTEMS: CURRENT THROUGH THIN FILMS.....	64
6.1. EXPERIMENTAL SETUP AND THE MEASUREMENT.....	64
6.2. THE ANALYSIS.....	66
7. q -GAUSSIAN ANALYSIS OF THE ELECTRONIC BEHAVIOR IN $AS_2S_3(AG)$ AND $AS_2SE_3(AL)$ THIN FILMS.....	72
7.1. THE ANALYSIS.....	72

8. CONCLUSION.....75

REFERENCES.....76



LIST OF FIGURES

Figure 2.1. The evolution of a system in spacetime	6
Figure 2.2. The state space of a system	6
Figure 2.3. Vector fields of representative systems	10
Figure 2.4. Time domain behavior of various two dimensional systems	10
Figure 2.5. Representative limit cycles.....	11
Figure 2.6. Examples of cycles represented in state spaces and graphs in time domain	12
Figure 2.7. An eigenplane and an eigendirection that together represent the behavior of a system	15
Figure 2.8. Lorenz system for different r values	16
Figure 2.9. Representation of the Lorenz attractor on the phase plane	18
Figure 2.10. Two trajectories varying 1 per cent in initial conditions.....	19
Figure 2.11. Two neighboring trajectories which separate in time	20
Figure 2.12. Horseshoe map	21
Figure 2.13. The Poincaré section method	23
Figure 2.14. Graphical iteration method.....	26
Figure 2.15. The Logistic map for different parameter r values	28

Figure 2.16. Graphical iterations and the cobweb constructions of the Logistic map for different parameter values	29
Figure 2.17. A period-I and a period-II orbits with Poincaré sections	30
Figure 2.18. Bifurcation diagram of the Logistic map	30
Figure 2.19. Two fixed points; a half-stable fixed point; and annihilation of the half-stable fixed point.....	32
Figure 2.20. The cobweb diagram of a period-II orbit	34
Figure 2.21. Two fixed points and a half-stable fixed point.....	36
Figure 2.22. A bifurcation diagram and a period doubling	37
Figure 2.23. N small square boxes in one square	39
Figure 2.24. The Cantor Set and the iterative evolution to it.....	41
Figure 2.25. The Chaos game board and the first three steps that are connected by line segments	42
Figure 2.26. The chaos game after 100 steps, 500 steps, 1000 steps and 10,000 steps.....	43
Figure 3.1. Mean squared displacement vs. time graph for different types of anomalous diffusion.....	47
Figure 4.1. q -Gaussian distribution	54
Figure 6.1. Schematic of the experimental setup.....	65
Figure 6.2. The data of $As_2S_3(Ag)$	66

Figure 6.3. The data of $As_2Se_3(Al)$	66
Figure 6.4. Correlation coefficient.....	67
Figure 6.5. Mutual information.....	68
Figure 6.6. False nearest neighbors	69
Figure 6.7. Largest Lyapunov Exponents with every line for $As_2S_3(Ag)$	69
Figure 6.8. Largest Lyapunov exponent with average line for $As_2S_3(Ag)$	70
Figure 6.9. Largest Lyapunov Exponents with every line for $As_2Se_3(Al)$	70
Figure 6.10. Largest Lyapunov exponent with average line for $As_2Se_3(Al)$	71
Figure 6.11. Hurst Analysis	72
Figure 7.1. PDF of the current magnitude differences for the transient current through thin $As_2S_3(Ag)$	75
Figure 7.2. PDF of the current magnitude differences for the transient current through thin $As_2Se_3(Al)$	75

LIST OF TABLES

Table 6.1. Lyapunov Exponents extracted from the data of $As_2S_3(Ag)$ and $As_2Se_3(Al)$ 71

Table 7.1. A , B and q parameter values of the fitted q -Gaussian function..... 75



LIST OF SYMBOLS/ABBREVIATIONS

$A(t)$	Auto-correlation function
D	Linearization operator
d_e	Embedding dimension
d_f	Box-counting dimension
$I(X; Y)$	Mutual information
J	Jacobian matrix
j	Diffusive flux
j_e	Electric current density
j_H	Heat current density
k	Iteration number
n	Number of the time steps
P	Poincaré mapping operator
$p_{qg}(x)$	Probability density function of the q -Gaussian distribution
S_{BG}	Boltzmann-Gibbs entropy
S_q	Generalized entropy
$S(\Delta n)$	Stretching factor
$S(t)$	One dimensional signal
t	Time
$U(s_{n_0})$	Neighborhood of s_{n_0}
W	Number of discrete states
x_f	Fixed point
$y(n)$	Integrated time series
$\vec{\delta}$	Separation vector
$\phi(x)$	Concentration of x
D	Diffusion coefficient
H	The Hurst exponent
λ	Lyapunov Exponent

FNN	False Nearest Neighbors
PDF	Probability density function
PEG	Poly Ethylene Glycol
PMMA	Polymethylmethacrylate



1. INTRODUCTION

Karl Popper, in his famous book *The Logic of Scientific Discovery*, says that he believes that there is a main philosophical problem which all thinking people are interested in: “The problem of cosmology: the problem of understanding the world –including ourselves, and our knowledge, as part of the world” [1]. He believes that all science is cosmology. Indeed, we can see the history of all kinds of sciences and philosophy as a part of understanding the world, or of cosmology.

In the very beginning of the history of western cosmology, as Hesiod tells, *chaos* was thought as the origin of the universe in the sense that the infinite crude and unshaped space which existed before the universe had converged with the harmony and order [2]. After over two thousands of years, we reclaim the word of *chaos* to be a part of our understanding the universe and nature. Chaos describes a disordered state, in general. However, in today’s science, chaos implies a deeper meaning that is going to be explained in more detail in the next chapters.

By the developments in nonlinear dynamics, many studies have been done; especially the interdisciplinary ones have found the chance to stand, since the nature behaves nonlinearly and it lives everywhere from biology, chemistry, physics to social movements, finance and atmosphere. Although the chaos theory is in its infancy stage, it seems to stand up and begin to walk in the future.

We aimed in this study to briefly review the theory of chaos and to study the possible chaotic behavior in the transient current through thin films made of $\text{As}_2\text{S}_2(\text{Ag})$ and $\text{As}_2\text{Se}_2(\text{Al})$. Such dielectric materials are known to show irregular current characteristics under constant electric field or voltage. In the present study, the current through the corresponding thin films as a function of time is analyzed for chaoticity. The data were taken by a computerized data acquisition system. We analyzed the data using time series analysis for chaoticity, and further analysis was done by the method of q -statistics.

The plan of the thesis is as follows: In chapter two, historical and theoretical background on the dynamics and the nonlinear dynamics are given. In chapter three, a brief theoretical review is given for the diffusion and the diffusion in condensed matter. In chapter four,

theoretical background of nonextensive statistical mechanics and the generalization of the classical statistical mechanics are given. In chapter five, theoretical background on the analysis methods of the nonlinear time series used in the present study is given. In chapter six, the experiment and the chaos analysis are presented. In the seventh chapter, q -Gaussian analysis of the data is presented. Finally, chapter eight contains the conclusion of the study.



2. NONLINEAR DYNAMICAL SYSTEMS

2.1. A BRIEF HISTORY OF DYNAMICS

For our modern understanding of physics, the first main step came by Newton's discoveries on differential equations, laws of motions and universal gravitation in the seventeenth century. He solved the two-body problem, specifically, the motion of the earth around the sun. After Newton, people put lots of effort on the table to solve the three-body problem. Approximately two hundred years passed with no remarkable achievements on the subject. Three-body problem seemed to be impossible to solve. In late 1800s, Poincaré showed that it cannot be solved.

In the nineteenth century, Poincaré suggested a new idea about the way of approaching this problem. Instead of asking the exact positions of the objects of a system in the space, he asked if the system is stable for all times or not. He developed a strong geometric approach for those kinds of system behaviors that are hard to handle. Poincaré did not discover chaos, but he prepared the ground.

Although chaos phenomenon was not discovered deeply, physicists' understanding of nonlinear oscillations played a great role for the technology. Many technological developments such as radio, radar, lasers etc. were achieved.

The developments of high-speed computers played a vital role in the studies of dynamics, because lots of data and calculations could be analyzed by the computers in a way which was not possible before. In the following period, 1920-1960, important scientists such as Birkhoff, Kolmogorov, Arnold and Moser made significant contributions in classical mechanics. They studied complex behavior in Hamiltonian mechanics. In 1963, Edward Lorenz, who was a mathematician in MIT, published his famous paper in a journal about atmospheric sciences: *Deterministic Nonperiodic Flow* [3]. He discovered the chaotic motion on a strange attractor. He studied on a simple system representing cellular convection and he solved it numerically. He found all the solutions were unstable and nonperiodic. He also observed the sensitive dependence on the initial conditions. If an even very small difference was made in the simulation, he found that the results became totally

different. He argued that the long term prediction is impossible for the chaotic systems whether the system is deterministic or not.

Since Lorenz's paper was published in a journal for atmospheric science, physicists and mathematicians did not realize it and its importance for a few years. In 1970s, some significant developments had come. Ruelle and Takens suggested a new theory about turbulence in fluids based on abstract considerations about the strange attractors. Robert May found examples of chaos in the logistic map of biological population growth. In 1978, Feigenbaum discovered the universal laws governing the transition from normal behavior to chaotic behavior. He made the connection between chaos and phase transitions. Experimental studies of chaos in fluids, electronic circuits, chemical reactions, mechanical oscillators etc. were done largely.

In late 1970s, Mandelbrot came with computer graphics of fractals and showed how they could be applied in different subjects. His quote which was the turning point of his thought has become famous: "How long is the coast of Britain?" [4]. His ideas about fractal geometry structured on this question, and as it can be seen on his fractal images, he came up with the point of view that implies the following: The distance of the coast depends on the dimension of the ruler.

1980s passed with widespread studies in chaos, fractals, oscillations and their applications.

1990s also passed more with engineering applications of chaos and complex systems.

In 2000s, chaotic studies in network systems (neural, economics, internet etc.) had dominant importance.

2.2. REPRESENTATION OF DYNAMICAL SYSTEMS

Everything we can think in the real world is a dynamical system; solar system, human body, a flying bee, everything. To be able to understand the systems and to be able to control them, we first need to translate the language of nature, the language of the natures of these systems to a language that we can understand and study on: mathematics.

There are two main types of expression for dynamical systems: *differential equations* for continuous time domains and *iterated maps* for discrete time domains. Through Newton, by differential equations we have come a long way in understanding and expressing dynamical systems. Differential equations are used in science and engineering studies, but by iterated maps, or in other name the difference equations, we developed our success in studying nonlinear systems. It was impossible to solve the problems of chaotic behavior by differential equations only.

A dynamical system can be represented simply as follows (1-D case):

$$\frac{dx}{dt} = f(x) \quad (2.1)$$

where x represents the space coordinates and t is the time. Although any system in the world is actually a three dimensional dynamical system; for instance a simple electrical circuit can be approached as a one dimensional dynamical system, a pendulum can be approached as a two dimensional one etc. In general, a system can be represented as a set of differential equations for each dimension:

$$\frac{dx}{dt} = f_1(x, y, z) \quad (2.2)$$

$$\frac{dy}{dt} = f_2(x, y, z) \quad (2.3)$$

$$\frac{dz}{dt} = f_3(x, y, z) \quad (2.4)$$

The right-hand-sides are arbitrary functions (linear or nonlinear). If all these together with sufficient initial or boundary conditions are defined, then we can say that the system is completely defined, and the problem is a well posed one.

A differential equation can be solved in two ways: explicitly or by numerical methods. Numerical solving gives an approximate solution. Here, the ways of solving are not going to be looked. The differential equation describes the evolution of the system in time. The solution may yield such a result as shown in the following figure:

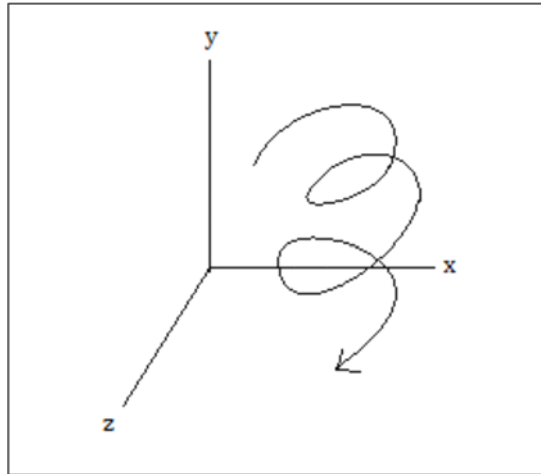


Figure 2.1. The evolution of a system in spacetime.

The trajectory begins at a chosen initial condition for all the coordinates. The evolution of the system at any point can be understood from the differential equation by placing the corresponding condition values as a new initial condition to the right-hand-side of the equation; the result shows how much evolution will be seen in each coordinate.

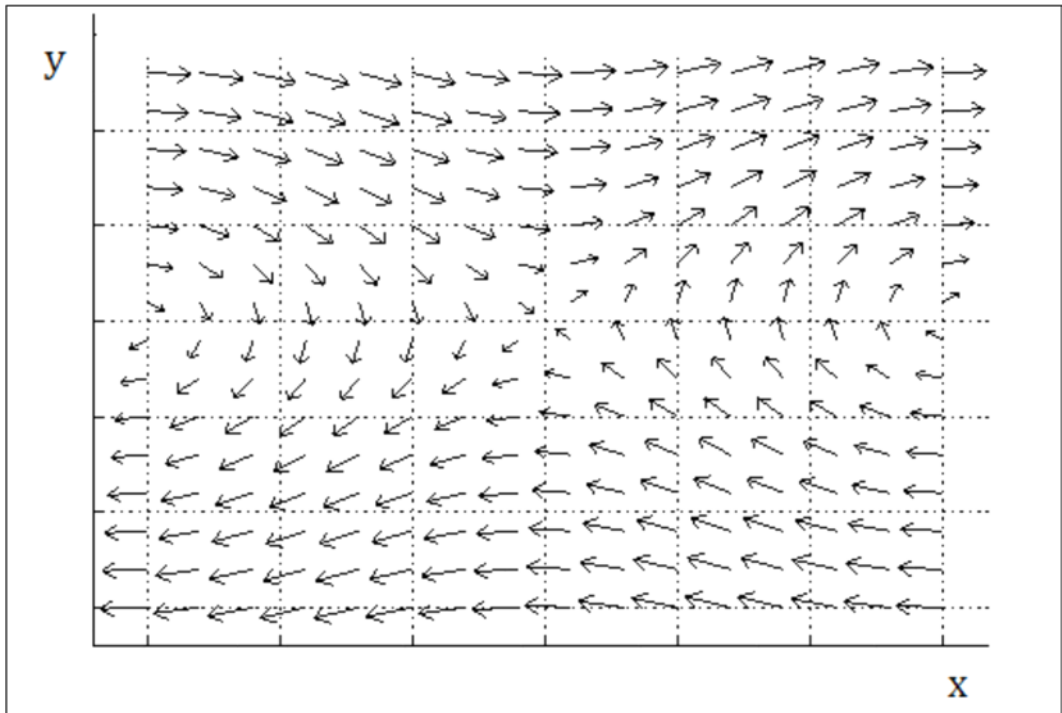


Figure 2.2. The state space of a system.

The differential equation describes an arrow at any point in *the state space* (Fig. 2.2). Thus, it can be known that for each point on the space to which direction the evolution takes place. This is determined by the system. In *the phase space*, there are arrows everywhere like a stream. Each point represents the behavior of the system in the phase space. Since it seems like a stream, set of differential equations are also called a *flow*. (There can be also a *sink* as we will look in the next pages.)

2.2.1. Linearization: A Tool to analyze the behaviors

Linearization (also known as linear approximation) method has been used as a very useful tool for the analysis of differential equations, particularly near an equilibrium point. Although it does not say anything about far points from the point that we interested in, for the understanding of the behavior of the system about the point, it gives a quick idea to us.

The technique can be described on an example system as following:

$$\dot{x} = f(x, y) \quad (2.5)$$

$$\dot{y} = g(x, y) \quad (2.6)$$

(The dot on the variable means that it is the first derivative with respect to time.)

If, say, (x_0, y_0) is an equilibrium point of the system, we can approximate and so find a closest linear system to our system around the point. To do this, the functions of the system can be expanded in series. Neglecting the terms higher than first order yields

$$f(x, y) \approx f(x_0, y_0) + \frac{\partial f}{\partial x}(x_0, y_0)(x - x_0) + \frac{\partial f}{\partial y}(x_0, y_0)(y - y_0) \quad (2.7)$$

$$g(x, y) \approx g(x_0, y_0) + \frac{\partial g}{\partial x}(x_0, y_0)(x - x_0) + \frac{\partial g}{\partial y}(x_0, y_0)(y - y_0) \quad (2.8)$$

Since (x_0, y_0) is the equilibrium point, $f(x_0, y_0) = g(x_0, y_0) = 0$. So the system is

$$\dot{x} = \frac{\partial f}{\partial x}(x_0, y_0)(x - x_0) + \frac{\partial f}{\partial y}(x_0, y_0)(y - y_0) \quad (2.9)$$

$$\dot{y} = \frac{\partial g}{\partial x}(x_0, y_0)(x - x_0) + \frac{\partial g}{\partial y}(x_0, y_0)(y - y_0) \quad (2.10)$$

The equations can be organized into a matrix equation and the coefficient matrix of the system would be then the Jacobian matrix. The Jacobian matrix is the matrix of all first-order partial derivatives of a vector-valued function.

By linearizing, we can investigate the stability of a system and get quantitative measures, for instance, the rate of decay etc.

Linearization is not enough to understand the world that we analyze every time. If, for instance, for this example, the terms that we neglect are not negligible, then we need some other techniques. Graphical methods are useful for such times.

2.3. PHASE PLANE AND VECTOR FIELDS

A phase space for a system is the space that includes all possible states of the system. Each possible state is represented by a point in the phase space. In a phase space, a two dimensional system is called a *phase plane*. Since each point can serve as an initial point, the phase plane is full of trajectories. Thus the phase plane is also seen as a *vector field*. It is usually impossible to get the trajectories analytically. So, for a more qualitative idea, the phase plane method is used.

Once the phase portrait of a system is found, four important features can be seen easily: the fixed points, the closed orbits, the behavior of the system near the fixed points and closed orbits, and the stability or instability of the fixed points and closed orbits.

A linear system can be expressed as

$$\begin{bmatrix} \delta\dot{x} \\ \delta\dot{y} \end{bmatrix} = \begin{bmatrix} \frac{\partial f_1}{\partial x} & \frac{\partial f_1}{\partial y} \\ \frac{\partial f_2}{\partial x} & \frac{\partial f_2}{\partial y} \end{bmatrix} \begin{bmatrix} \delta x \\ \delta y \end{bmatrix} \quad (2.11)$$

and can be solved analytically. More often, they are solved with the coefficients of the right hand side written in matrix form, known as the Jacobian matrix, using eigenvalues λ , given by the determinant (known as *the characteristic equation*),

$$\det(J - \lambda I) = 0 \quad (2.12)$$

where the J is the Jacobian matrix; with eigenvectors

$$J\vec{x} = \lambda x. \quad (2.13)$$

The general solution is:

$$x = \begin{bmatrix} k_1 \\ k_2 \end{bmatrix} c_1 e^{\lambda_1 t} + \begin{bmatrix} k_3 \\ k_4 \end{bmatrix} c_2 e^{\lambda_2 t} \quad (2.14)$$

where λ_1 and λ_2 are the eigenvalues, and (k_1, k_2) , (k_3, k_4) are the basic eigenvectors, c_1 and c_2 are arbitrary coefficients. The characteristic equation yields

$$\lambda^2 - \tau\lambda + \Delta = 0, \quad (2.15)$$

where

$$\tau = \text{trace}(J), \quad (2.16)$$

$$\Delta = \det(J). \quad (2.17)$$

Thus, the explicit solutions for the eigenvalues are written as

$$\lambda = \frac{1}{2}(\tau \pm \sqrt{\tau^2 - 4\Delta}) \quad (2.18)$$

The eigenvectors and the nodes determine the profile of the trajectories on the vector field.

According to the eigenvalues, the systems manifest themselves as follows:

- i. If any $\lambda > 0$, the system is *unstable* (Fig. 2.3.a);
- ii. if all $\lambda < 0$, the system is *stable* (Fig. 2.3.b);
- iii. if $\lambda_1 > 0$ and $\lambda_2 < 0$, the origin would be a *saddle point*, that is, the first eigensolution grows exponentially while the second one decays (Fig. 2.3.c);
- iv. if eigenvalues are complex, then the fixed point either a *center* (Fig. 2.3.d) or a *spiral* (Fig. 2.3.e and Fig. 2.3.f). The spirals can either be a *source* (Fig. 2.3.e) or a *sink* (Fig. 2.3.f).

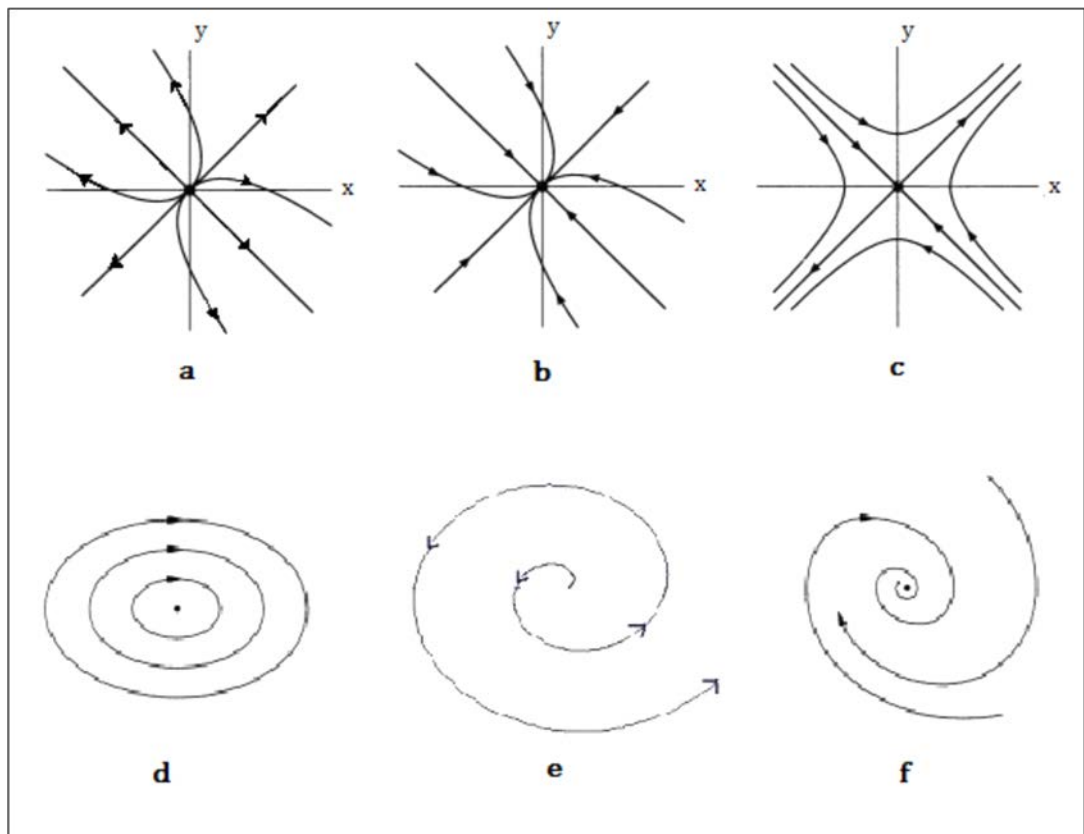


Figure 2.3. Vector fields of representative systems.

In the following representative graphs (Figure 2.4.a, b, c), the behaviors of the systems in Figures 2.3.d, e, f can be seen in time domains respectively:

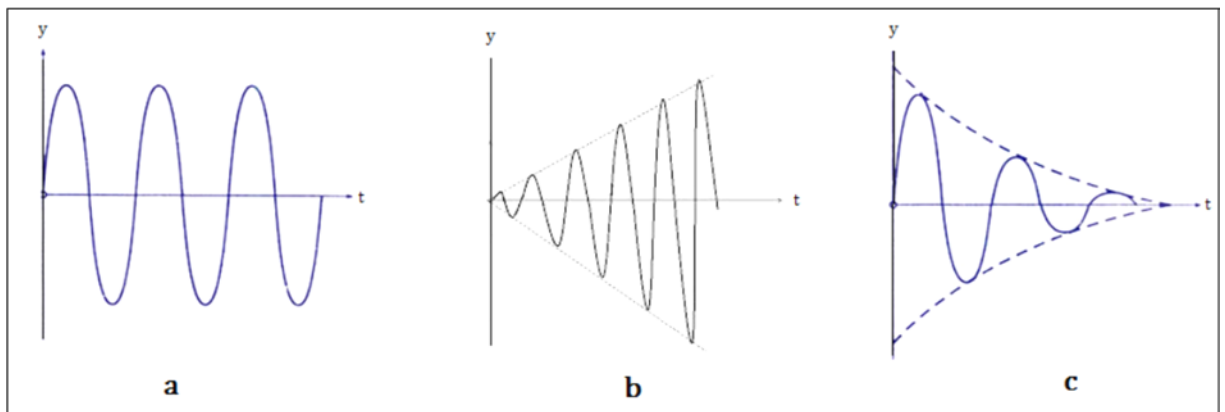


Figure 2.4. Time domain behavior of various two dimensional systems.

2.4. LIMIT CYCLES

How can two spirals be nested? The only possibility of such a situation is that there is a *limit cycle* between them. A limit cycle is an isolated closed path. It is isolated, because neighboring paths are not closed. If all the neighboring trajectories approach to the limit cycle as time approaches infinity, it is called a *stable* limit cycle (also called as *attracting* limit cycle) (see Fig. 2.5.a). In the reverse situation the limit cycle is *unstable* (Fig. 2.5.b). If there is a neighboring trajectory which spirals into the limit cycle as time goes infinity and another one which spirals into the origin or moves away from the limit cycle as time goes infinity, then it is a *half-stable* limit cycle (Fig. 2.5.c).

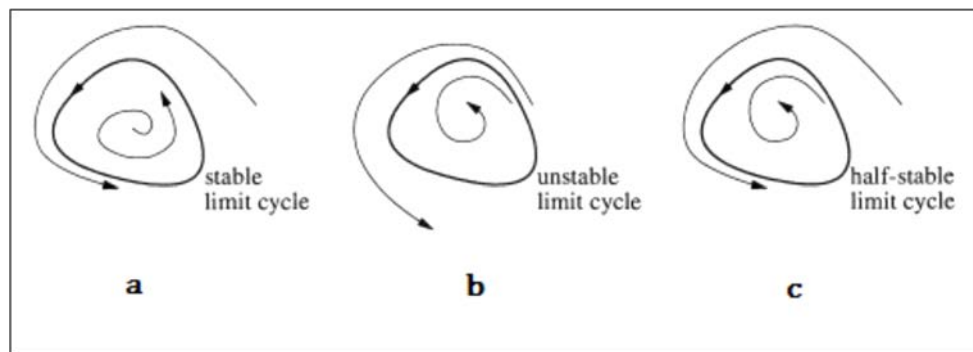


Figure 2.5. Representative limit cycles [5].

Stable limit cycles are examples of attractors and they are very important in life. For instance, if our heart's behavior would not have a limit cycle, it will not go back to its normal rhythm once we run. The difference between the limit cycles and the normal closed orbits is that any small perturbation given to the system results with return of the system to the standard cycle (limit cycle). In closed orbits, if any perturbation is given to the system, the system goes to a new orbit and stays there until any other perturbation will be given. The limit cycle phenomenon shows how stable oscillations are created in nature. Although sinusoidal periodic oscillations are characteristic of linear systems, stable oscillations with multiple periodicities that depend on the amplitude are usually characteristics of nonlinear systems.

For a better understanding some examples of cycles are given by the representative figures below:

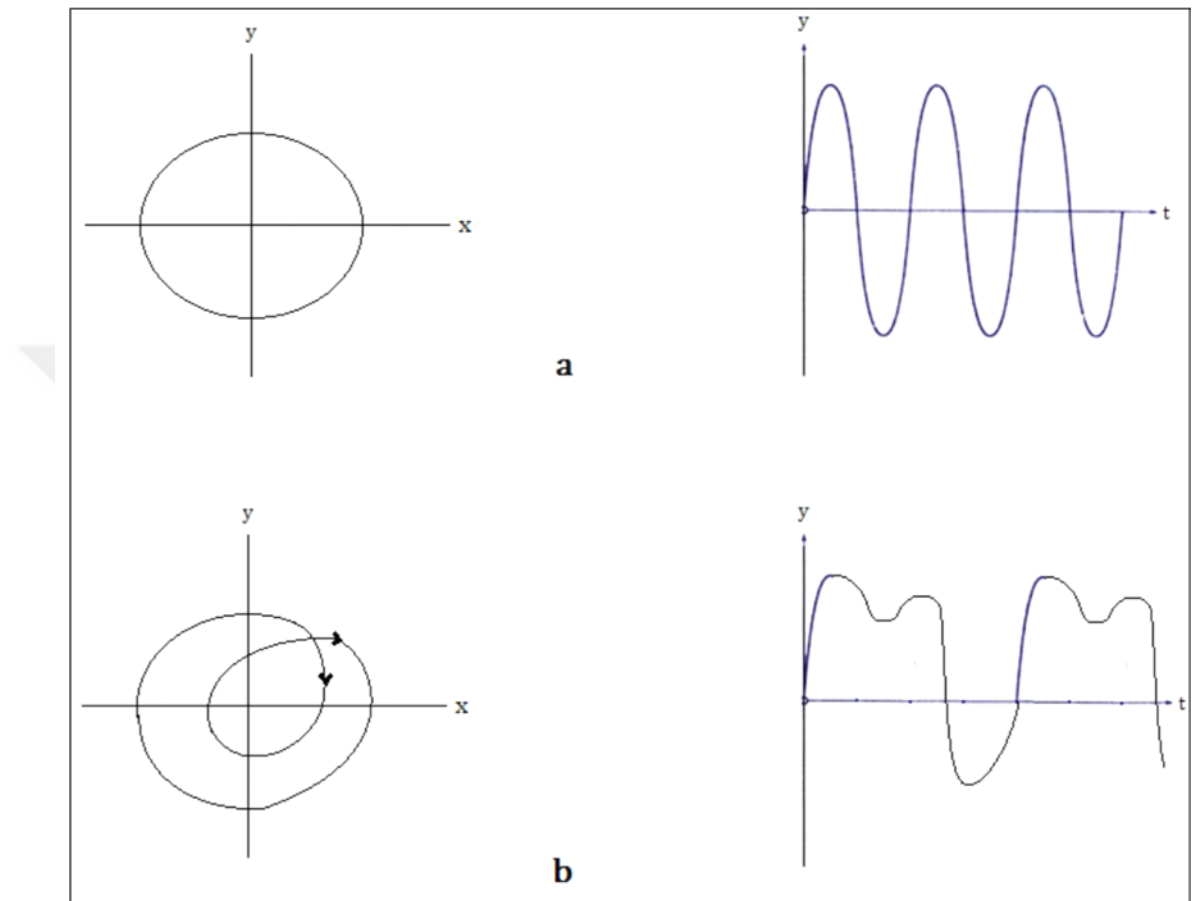


Figure 2.6. Examples of cycles represented in both state spaces and graphs in time domain.

In Fig. 2.6.a, a normal closed orbit and its behavior in time domain are given; in Fig. 2.6.b, a period-II limit cycle is given. Of course, it is just a projection of a period-II limit cycle, since such a cycle can only occur in three-dimension; because, there cannot be two arrows in one point, or trajectories cannot overlap (existence and uniqueness theorem). There can also be period-“more-than-two” limit cycles. Period infinity orbit is also possible. Period infinity means that it never comes to itself, or comes to itself at infinity. Bounded periodic infinite orbits imply the chaos as it will be seen in the following chapters.

2.5. ATTRACTORS I: LORENZ SYSTEM

In real physical world, any dynamical system is a dissipative system. The dissipation and the driving force tend to cancel out the system into its normal behavior. The subset of the phase space of the dynamical system corresponding to the normal behavior is the *attractor*. Actually, a strict mathematical definition of an attractor has not been universally agreed upon. However, in other words, it can be said that an attractor is a set of properties toward which a system tends to evolve, no matter what the initial conditions of the system are. Mathematically speaking, it can be said that this is the invariant subset A of a phase space \mathbb{R}^n of the differential equation

$$\frac{dx}{dt} = f(x), \quad (2.19)$$

where $x \in \mathbb{R}^n$, which is approached as time goes to infinity, is called an *attractor*. An attractor can be a point, a finite set of points, a curve, a manifold or even a complicated set with a fractal structure known as a strange attractor.

2.5.1. Lorenz Equations

In 1963, the M.I.T. meteorologist Edward Lorenz developed a simplified model of convection rolls in the atmosphere. He developed the equations of his system as a model for the modal amplitudes in a nonlinear thermal convection problem, as it was said. Lorenz discovered that for some values of parameters, the solutions of the equations of the system exhibit an unusual form of behavior that is called *chaos* today.

The Lorenz equations:

$$\dot{x} = \sigma(y - x), \quad (2.20.a)$$

$$\dot{y} = rx - y - xz, \quad (2.20.b)$$

$$\dot{z} = xy - bz, \quad (2.20.c)$$

where σ , r and b are positive parameters.

The equilibrium points of the system are

$$A = (0,0,0), \quad (2.21)$$

$$B = (\sqrt{b(r-1)}, \sqrt{b(r-1)}, (r-1)), \quad (2.22)$$

$$C = (-\sqrt{b(r-1)}, -\sqrt{b(r-1)}, (r-1)). \quad (2.23)$$

If r is less than 1, $\sqrt{b(r-1)}$ is imaginary. The position of the equilibrium point must be real, so 1 is a critical value for r . That is, when r is less than 1, the equilibrium points B and C do not exist. Once r reaches the value 1, B and C appear. The point A is always there as it can be seen. If one wants to say more about the behavior of the system, stability analysis of the equilibrium points is needed.

Jacobian matrix of the system is given by

$$J = \begin{bmatrix} -\sigma & \sigma & 0 \\ -z+r & -1 & -x \\ y & x & -b \end{bmatrix} \quad (2.24)$$

The matrix simplifies to the following one at $(0,0,0)$: (A) ;

$$J = \begin{bmatrix} -\sigma & \sigma & 0 \\ r & -1 & 0 \\ 0 & 0 & -b \end{bmatrix} \quad (2.25)$$

Lorenz took the parameter values as $\sigma = 10$ and $b = \frac{8}{3}$. The parameter r can be changed and the change in behavior of the system may be observed. If the parameter values of σ and b are substituted and the eigenvalues are calculated, we get the following three eigenvalues:

$$\lambda = -\frac{8}{3}, \frac{-11 \pm \sqrt{81+40r}}{2} \quad (2.26)$$

All the eigenvalues are real (note that the parameters were assumed as positive), and this means that any motion starting at any point will go to the equilibrium point, even if the

system is unstable. For r values less than 1, as it was specified, only the point A exists. When r reaches 1, other two equilibrium points come into play and the point A loses its stability. A becomes unstable, but in a specific way. In a particular direction it is unstable, the direction along the corresponding eigendirections. To understand which directions they are, one needs to calculate the new eigenvalues for the new equilibrium points.

If the Jacobian matrix is calculated (for the same σ and b) for the point B , we get the following, say, for $r = 1$:

$$J = \begin{bmatrix} -10 & 10 & 0 \\ 1 & -1 & -\sqrt{8/3} \\ \sqrt{8/3} & \sqrt{8/3} & -8/3 \end{bmatrix} \quad (2.27)$$

It yields three eigenvalues; one is real and negative and other two are complex conjugates with negative real parts. The other equilibrium point shows a similar result. The complex conjugate eigenvalues imply that there is an eigenplane lying in the space. The real and imaginary parts of the corresponding eigenvectors individually give solutions. The real part is simply a vector in the real space, and the real part of the imaginary part is also a real vector. Thus, a unique plane lies in the space which passes on these two vectors. Hence, there is an eigenplane coming from the two eigenvalues which are complex conjugates and there is an eigendirection coming from the real eigenvalue. It can be shown representatively in the following figure:

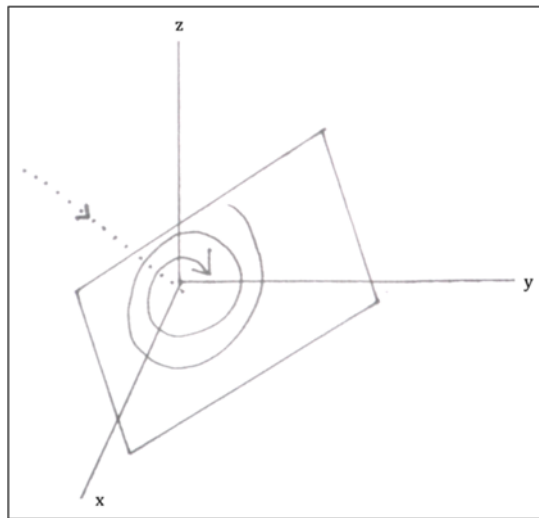


Figure 2.7. An eigenplane and an eigendirection that together represent the behavior of a system.

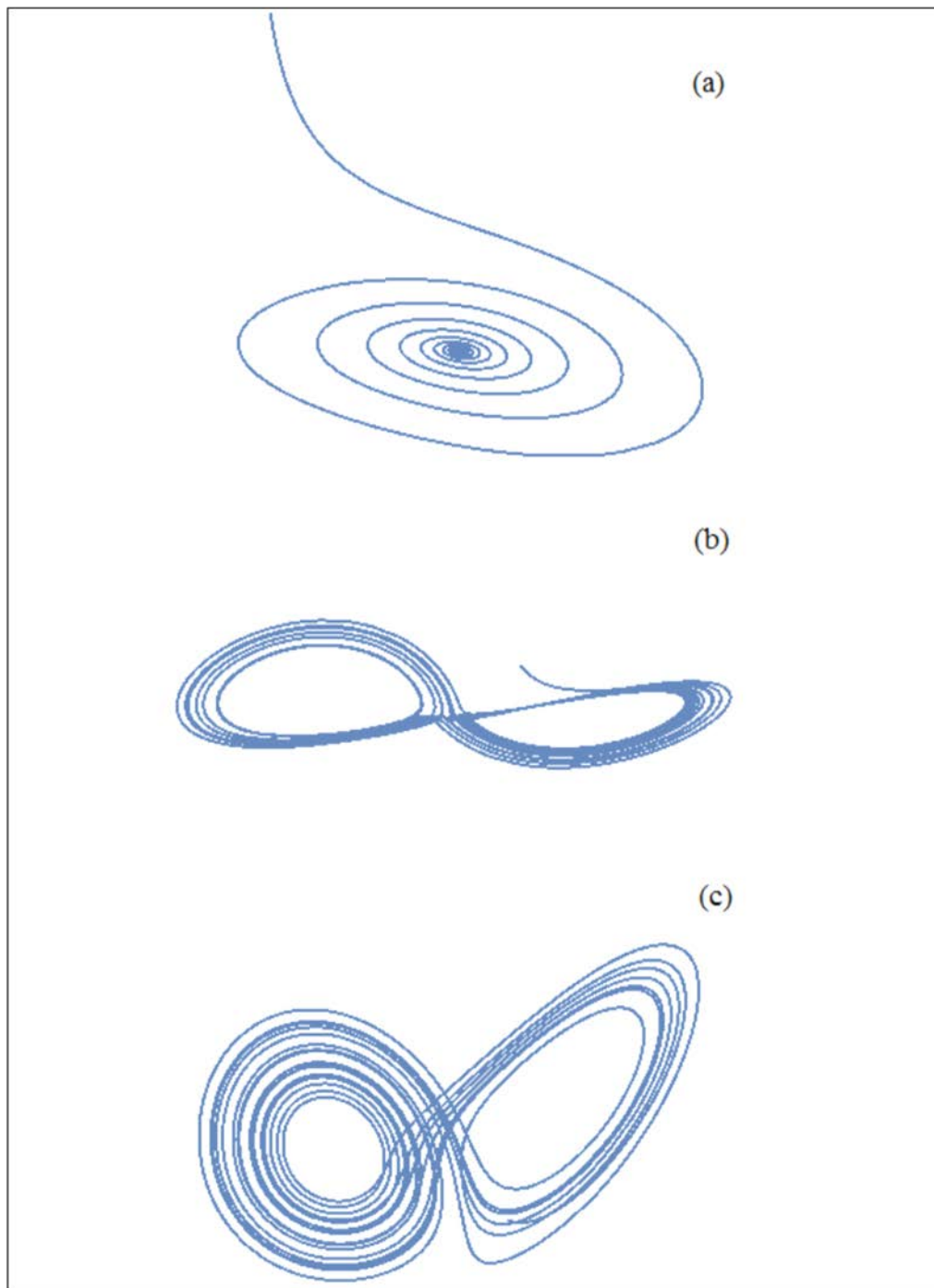


Figure 2.8. Lorenz system for different r values. Initial conditions are chosen arbitrarily to be $x_0 = 1$, $y_0 = 8$, $z_0 = 10$, and they are the same for each graph. Parameters b and σ are also same for each graph and $8/3$ and 12.03 respectively; r is 13.04 in (a), 20.5 in (b) and 30 in (c) [6].

If any motion begins in the eigenplane, it stays on the plane and approaches the equilibrium point by a spiral trajectory. Any motion starting at a point out of the plane approaches the equilibrium point by a spiral trajectory that goes along the eigendirection. That is, the trajectory will be like a helix.

There are two equilibrium points for r values greater than 1; and so, there are two regions similar to each other. That is, two eigenplanes, two attractors exist. What happens to a motion that starts at any point in the space between these two attractors? Which one will be able to attract the motion? At this point an important concept is needed to be determined: *basin of attraction*. The basin of attraction of an attractor is the set of initial conditions leading to long-time behavior that approaches that attractor. So, here, the fate of the motion depends on the basin of attraction that the motion initially lies in. As the parameter r changes, the stable equilibrium points can lose their stability. The spirals that point outward can be formed and also the two eigenplanes that approach each other can overlap. Transitions can be observed from one plane to other one. Chaos can be formed. Figure 2.8 represents the Lorenz system for different r values.

2.6. ATTRACTORS II: STRANGE ATTRACTORS

The term *strange attractor* was coined by David Ruelle and Floris Takens [7]. The attractor they studied had a fractal structure, that is, a strange structure. “What is a fractal set?” is the question that we are planning to clarify in the following chapters. Although nonchaotic strange attractors also exist [8], usually a chaotic behavior is observed on a strange attractor. In simply saying, a strange attractor is an attractor that shows sensitive dependence on initial conditions. There are of course, many strange attractors like Rössler attractor, Henon attractor etc. Lorenz attractor is one of the basics.

2.6.1. Lorenz Attractor

Lorenz wanted to study on long term predictions on weather. He concluded after his study that long term prediction is very difficult.

He used numerical integration to observe the behavior in long term. As it was stated in the previous chapter, the parameters he chose were $\sigma = 10$, $b = \frac{8}{3}$ and $r = 28$. This value of r is the one that is just beyond the value for a fixed point that loses its stability as a pair of complex conjugate eigenvalues of the linearization around the corresponding fixed point. Such a phenomenon is called a bifurcation. Bifurcations are going to be reviewed in section 2.9, here, instead, the main idea beyond the strange attractor is going to be given. As it was given before, after an r exceeds a value, the origin loses its stability and turns into a saddle point. Lorenz started his calculations (or iterations) from a point very near to this saddle point at the origin. He saw after a suitable time that the motion is an *aperiodic* motion. He discovered that the motion exhibits an interesting view on the phase plane. If one looks to the geometry of the system on the phase plane, for instance towards $x - z$ plane, one sees a “pattern that looks like a butterfly (see Figure 2.9).

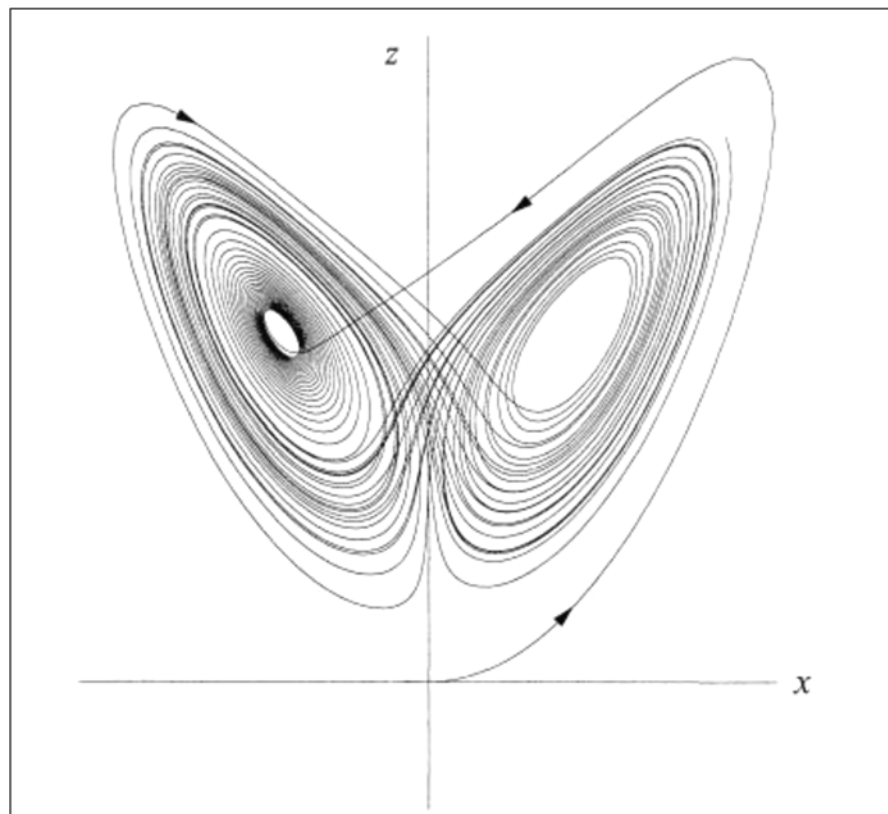


Figure 2.9. Representation of the Lorenz attractor on the phase plane [5].

As it is stated in section 2.5.1., the two attractors overlap and form a new type of an attractor. The trajectory starts somewhere, for instance, as in the figure, near the origin, goes to the right and dives into the center of the left one, then stays a little bit of time and goes again to the right, and so on. The number of turns that the trajectory makes on either side is not certain. The behavior seems like a random process. However, it is not. The system is actually deterministic.

2.6.2. Sensitive Dependence on Initial Conditions and Chaos

When Lorenz ran the computer program to calculate his weather model again, he observed that the result were completely different. An even very small difference at the initial conditions gave totally different outcomes. Lorenz discovered that a pair of nearby trajectories can be found in later times at very different locations on the attractor. The effect was coined by him as *sensitive dependence on initial conditions*. This phenomenon is one of the main characteristics of chaos. Also, that phenomenon is the main reason why long term predictions about weather cannot be made. Figure 2.10 shows that two trajectories varying 1 percent in initial conditions exhibit immensely different behaviors after sometime.

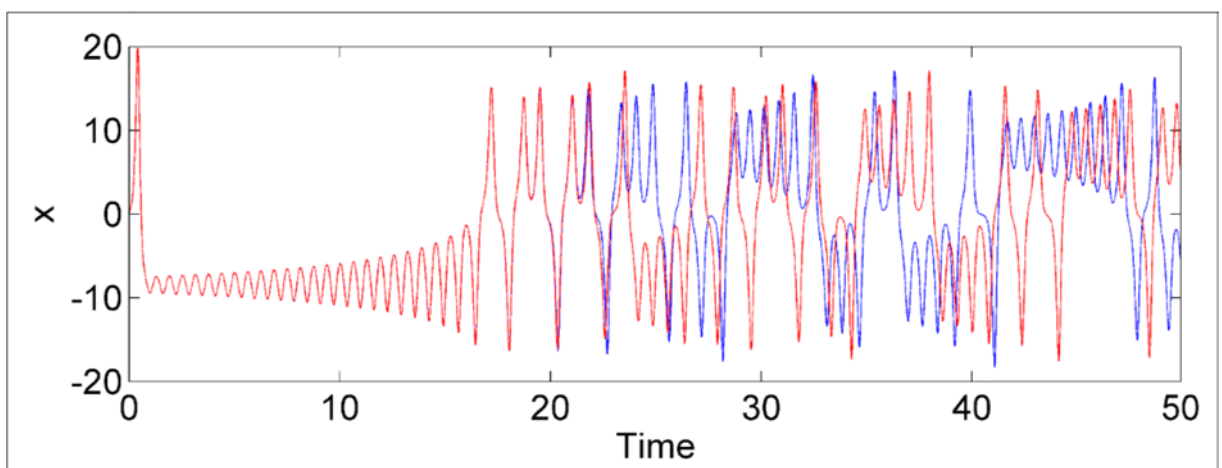


Figure 2.10. Two trajectories varying 1 per cent in initial conditions [9].

To make it clear, a mathematical interpretation would be better. If $\vec{x}(t)$ is a point on the attractor at time t and $\vec{x}(t) + \vec{\delta}(t)$ is a nearby point, where $\vec{\delta}$ is a small separation vector of initial length for instance $\|\vec{\delta}_0\| = 10^{-15}$. Lorenz found in his numerical studies that $\vec{\delta}$ grows exponentially fast with time in the appropriate direction (see Fig. 2.11):

$$\|\vec{\delta}(t)\| \cong \|\vec{\delta}_0\| e^{\lambda t}, \quad (2.28)$$

where $\lambda \cong 0.9$ [5].

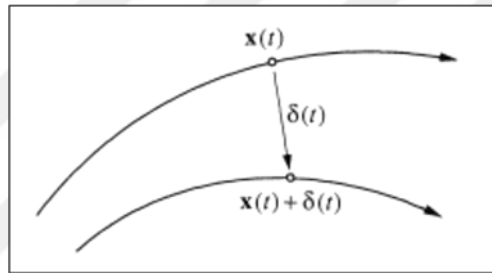


Figure 2.11. Two neighboring trajectories which separate in time [5].

2.6.2.1. Lyapunov Exponent

As quantitatively seen above, in mathematics, the Lyapunov exponent (named after Aleksandr Lyapunov) of a dynamical system is a quantity that describes the rate of separation of infinitesimally close trajectories. That is, for Eq. 2.28, λ is the Lyapunov exponent. Although it is often called Lyapunov exponent, it is actually the Maximal Lyapunov exponent. The rate of separation can vary for different initial separation vectors. So, there is a spectrum of Lyapunov exponents and the number of these equal to the dimensionality of the phase space. Any $\vec{\delta}_0$ will typically contain some component in the direction associated with the Maximal Lyapunov exponent, and because of the exponential growth rate of it, the effect of the other exponents will seem like zero by the time. That is why the Maximal Lyapunov exponent is used as an indication for identifying the system if it is chaotic or not. If it is positive, the system is chaotic.

In such a situation, there presents a *time horizon* that indicates the time border which the things will be complicated beyond it. That is, the separation $\vec{\delta}(t)$ will be so high that no prediction can be done any more after this time. Time horizon is given as

$$t_{horizon} \cong O\left(\frac{1}{\lambda} \ln \frac{a}{\|\vec{\delta}_0\|}\right). \quad (2.29)$$

Since the time logarithmically depends on initial separation $\|\vec{\delta}_0\|$ even if the initial measurement errors are very small, after a couple of times of $1/\lambda$, the prediction fails [5].

2.6.2.2. Smale's Horseshoe

Stephen Smale suggested thinking in a geometric way in order to understand the behavior of the strange attractors while he was studying the behavior of the orbits of the van der Pol oscillator [10]. Smale asked how the trajectories on the attractor endure in limited or bounded region of phase space while they continue to separate from neighboring trajectories. He introduced the *horseshoe* map that tells the mechanism of chaotic maps. The action of the map can be summarized in two words: stretching and folding.

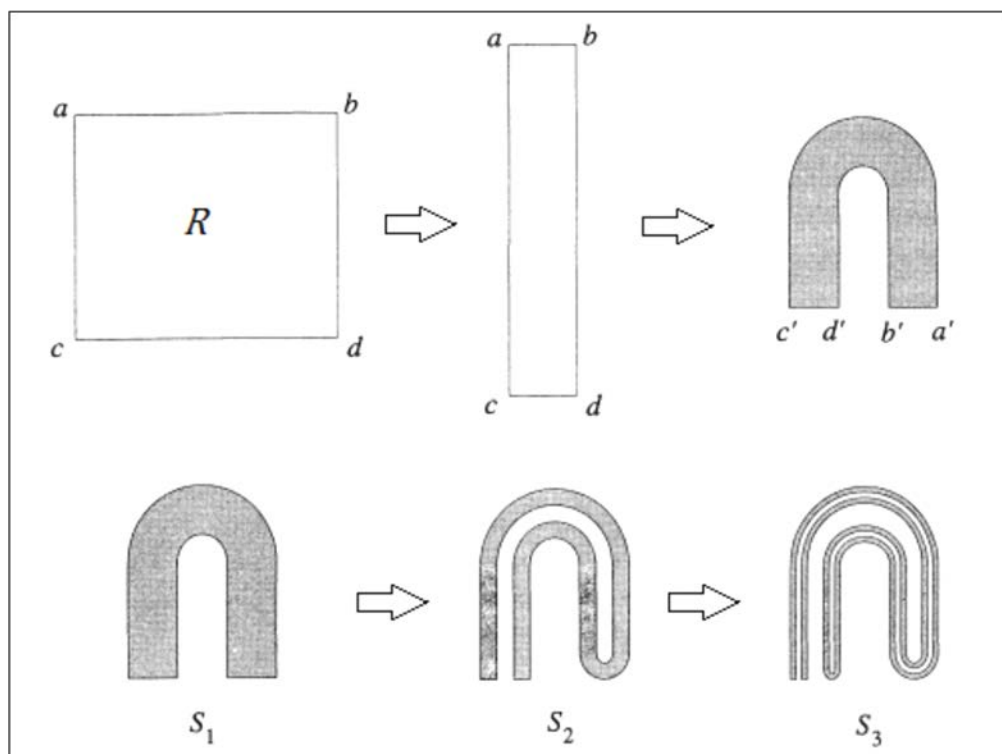


Figure 2.12. Horseshoe map [5].

For instance, if we take a region R determined by the rectangle $abcd$ (Fig. 2.12) and stretch it, we get a thin and long rectangle. If we fold the new rectangle as in Fig 2.12, we get a shape like a horseshoe. Here the horseshoe map does the action stitching and folding. If we keep going the same procedure, the region R will be preserved in a very long and thin shape as S_1 , S_2 , and S_3 etc. If a horizontal cross section is taken of the resulting set S_∞ , which is the limiting set of the mapping that is done infinitely many times, a Cantor set would be obtained.

As a result, for a horseshoe map, we can say that there are infinitely many periodic orbits whose number grows exponentially with the period; sensitive dependence of initial condition can be observed; the region is still kept bounded.

2.6.2.3. Chaos

As Strogatz says in his book [5], there is no universally accepted definition of chaos yet. However, we can say that “*chaos* is aperiodic long-term behavior in a deterministic system that exhibits sensitive dependence on initial conditions”.

An attractor is a set where all neighboring trajectories converge to. If the behavior is sensitively dependent on initial conditions, then we call the attractor as a strange attractor, and there is chaos on the attractor.

2.7. DISCRETE-TIME DYNAMICAL SYSTEM

In reality, the time is continuous and so the behavior of the real dynamical systems, although some of them exhibits a behavior like it is in discrete-time steps. Even the dynamical systems are in continuous time, it is easier to handle them on the paper (or computer) as taking them in a mathematical formalization that makes it discrete-time dynamical system. It is clear that to work with an equation like

$$x_{n+1} = f(x_n) \quad (2.30)$$

is easier than to work with an equation like Eq. 2.1.

A discrete-time dynamical system is actually a dynamical system, as stated above, whose state exhibits an evolution over state space in discrete-time steps. This evolution can occur

smoothly over time or in discrete-time steps. When a system is modeled as a discrete dynamical system, a snapshot of the system at a sequence of times is imagined. The snapshots may exist once a year, once every millisecond etc. The snapshots imply actually the variable that defines the state of the system.

2.7.1. Poincaré Maps

To find out the stability of an orbit like the one in Figure 2.13.a, we have a useful method which was suggested by Poincaré. It is supposed that there is an imaginary plane in the state space that intersects with the orbit. Any trajectory near that orbit in the state space can pass through the imaginary plane and there occurs, say, dots where the trajectories intersect with the plane. The following is clear: If the orbit in Figure 2.13.a is a stable orbit, any motion that can start near it, as in Figure 2.13.b, will approach to that closed orbit, and the intersection dots of the trajectories will also converge to the point of intersection that belongs to the corresponding orbit. The imaginary plane is called as Poincaré section. The sequence of points can be considered as a map derived from the orbit.

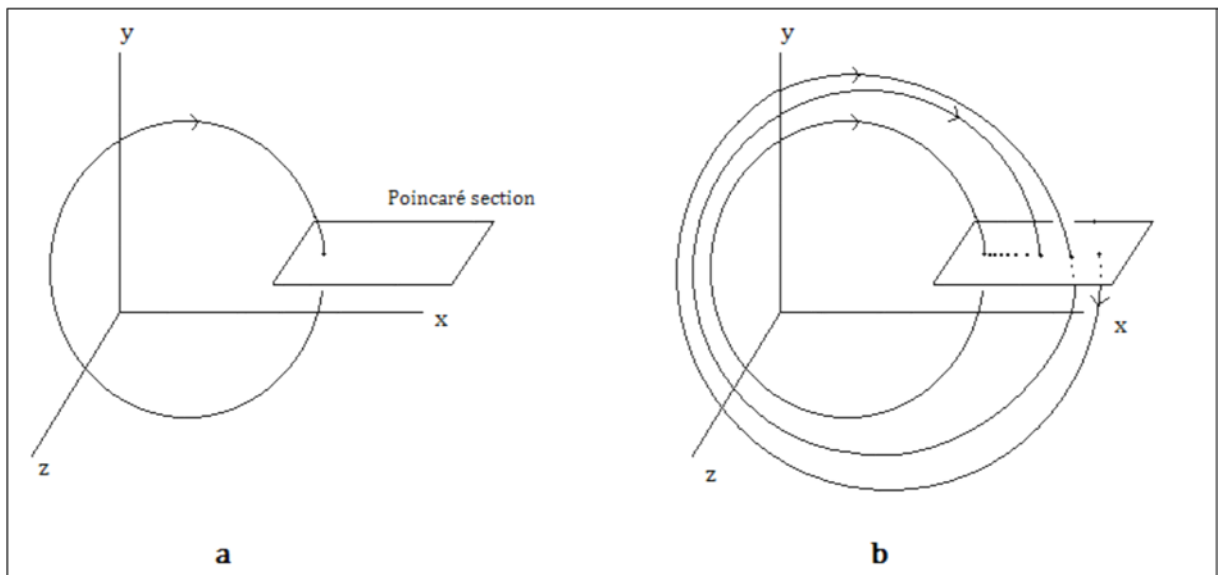


Figure 2.13. The Poincaré section method.

The Poincaré section method thus takes the continuous time orbit to the level of map, discrete-time phenomena. For the sake of mathematical language, Poincaré mapping can be defined as follows:

Let $\dot{\vec{x}} = f(\vec{x})$ be an n -dimensional system and let S be an $n - 1$ dimensional surface of section (Poincaré section) that transverse to a flow. *The Poincaré map*, P is a mapping from S to itself, obtained by iterative paths from one intersection with S to the next. If $x_k \in S$ is the k 'th intersection, then the Poincaré map is

$$\vec{x}_{k+1} = P(\vec{x}_k). \quad (2.31)$$

Note that if there is such a point \vec{a} that gives the result $P(\vec{a}) = \vec{a}$, then it is a fixed point which implies that if a trajectory starts at \vec{a} , it comes back to itself [5].

If there is a problem about closed orbits which is hard to handle, it usually becomes easier by this method as it turns into a problem about fixed points of mapping. Essentially, this method transforms a differential equation to a form of Eq. 2.30, or transforms a flow to a map. By this simplifying method, a difficult problem that includes complicated nonlinearities can be reduced to another problem. The local linear neighborhood of the map (for instance Fig. 2.13.a) and the stability of this fixed point can be analyzed as doing it for an equilibrium point.

2.7.1.1. Stability of Periodic Orbits

To analyze stability of periodic orbits, there are two widely used methods which are going to be given respectively; linear stability analysis and the cobweb construction.

Linear Stability Analysis: As stated above, the stability of periodic orbits can be analyzed by the linear stability approach that is achieved by the mapping method. There are two types of systems: Autonomous and non-autonomous. First one implies that there is no time dependence and the second one means that there is time dependence. First, stability of autonomous systems is going to be given, then the latter.

If a system $\dot{\vec{x}} = f(\vec{x})$ with a closed orbit is wanted to be analyzed, the corresponding fixed point \vec{x}_f of the map can be analyzed just as the methods used in chapter 2.3.

Suppose $P(\vec{x}_f) = \vec{x}_f$ is the Poincaré map of the fixed point. The linearization of the map about \vec{x}_f is

$$\xi_{k+1} = DP(\vec{x}_f)\xi_k. \quad (2.32)$$

If all eigenvalues of DP are less than one, then the fixed point x_f is asymptotically stable, and so is the corresponding periodic orbit. If so, then the fixed point x_f is an attractor of the map, and the periodic orbit is an attractor of the vector field. The other possibilities of the analysis go by the rules defined in the end of the section 2.3. In addition, there is one-to-one correspondence between the actual trajectories in the state space and their mappings, their projections on the Poincaré map: For example, if there are two stable points, then there is a period-II periodic orbit; if there are three stable points, that means there is period-III periodic orbit; and if there are infinitely many stable points, then there is a chaotic orbit.

For non-autonomous case, let's suppose a vector field

$$\frac{dx}{dt} = f(x, t), \quad (2.33)$$

where $f(x, t) = f(x, t + \tau)$; τ is some positive real number. Stability properties of a periodic orbit with period $T = a\tau/b$, where a and b are integers, can be found by considering a map such that it does the following:

$$x(t) \rightarrow x\left(t + \frac{a\tau}{b}\right). \quad (2.34)$$

From the eigenvalues of the map, we can determine the stability properties. We know that a point on a period- k periodic orbit of the map P is a fixed point of the map P^k . Hence, this fixed point of P^k and the periodic orbit of the map P have the same stability properties.

The Cobweb Construction: The construction takes its name from a theorem which is an economic model named by Nicholas Kaldor [11]. The method enables us to study a system graphically. The iteration of the map can be done graphically. By cobwebs, the global behavior of the system can be seen easily, and the other important usefulness of it is that in

such situations that the linear stability fails, by cobwebs the analysis can be done. An example to such a situation can be the following:

The linear stability fails in such a map as follows:

$$x_{k+1} = \sin x_k \quad (2.35)$$

The eigenvalue at fixed point $x_f = 0$ is $\lambda = f'(0) = \cos(0) = 1$, where f' is the derivative of f , the function $\sin(x)$. If the eigenvalue is greater than 1, then the fixed point is unstable. However, since the equal-to-1-eigenvalue means that the neglected terms in linearization determine the local stability, the linearization says nothing for the $\lambda = 1$ case. However, it can be seen by cobweb construction in Figure 2.14.b that $x_f = 0$ is a locally stable fixed point.

For a better understanding, the construction is given in two figures; one is (Fig. 2.14.a) to construct to concept, other one is (Fig. 2.14.b) to conclude the example. Consider P as any Poincaré map, and its graph is like in Figure 2.14.a. A fixed point x_f occurs at the point that the graph of the map intersects with the 45° line. By the graph, the iteration of the map could be done easily: Suppose x_k is an any point; if a vertical line is drawn from it until it intersects with the graph of the map, the intersection gives on the other axis the corresponding output x_{k+1} . If this last output is thought as a new input and a horizontal line at this time is drawn as in the previous situation and then the similar process is repeated, the cobweb construction method works.

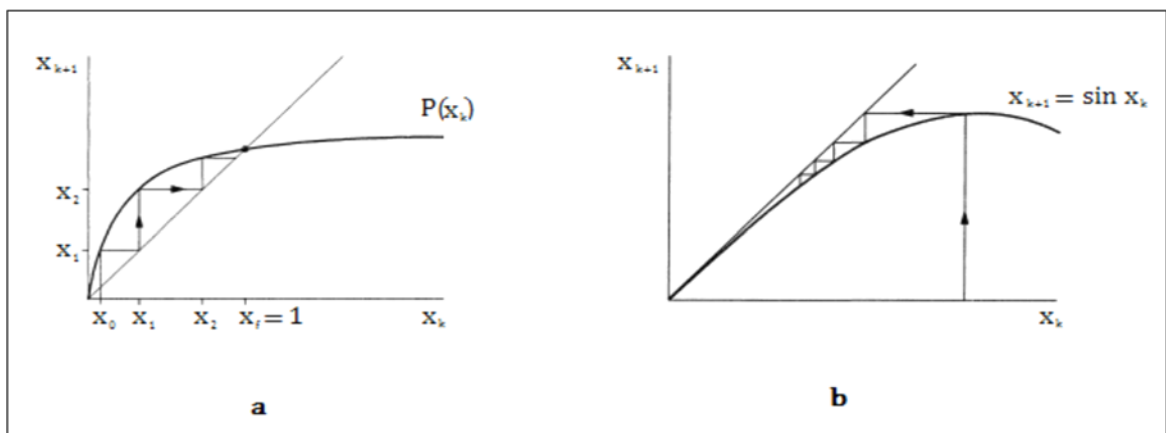


Figure 2.14. Graphical iteration method [5].

Now, the conclusion for the example can be seen as it has been explained if the graphical iteration is done in Fig. 2.14.b.

2.7.2. Lyapunov Exponent for 1-D Maps

Previously, in part 2.6.2.1, Lyapunov exponent was introduced to analyze the sensitive dependence on initial conditions. Here it is going to be revisited and its definition is going to be extended to 1-D maps. The advantage of 1-D maps is that they are easily visualized, that is, they are easy to draw.

As it is seen in Equation 2.28, the separation between the initially chosen points becomes after a time t , a value that depends on the time and the Lyapunov exponent exponentially. Now, it is to be thought as not “after a time”, but after a number of iteration; and not “depends on time”, but depends on the iteration number. Eq. 2.28 becomes

$$|\delta_k| \cong |\delta_0|e^{k\lambda}. \quad (2.36)$$

Here also a positive Lyapunov exponent implies chaos.

For more useful equation for the exponent, the derivation is as follows:

$$\log(|\delta_k|) \cong \log(|\delta_0|e^{k\lambda}) \quad (2.37)$$

$$\Rightarrow \lambda \cong \frac{1}{k} \ln \left| \frac{\delta_k}{\delta_0} \right| \quad (2.38)$$

$$= \frac{1}{k} \ln \left| \frac{f^k(x_0 + \delta_0) - f^k(x_0)}{\delta_0} \right|.$$

Taking the limit $\delta_0 \rightarrow 0$ gives

$$\lambda \cong \frac{1}{k} \ln |(f^k)'(x_0)|. \quad (2.39)$$

If the term in logarithm is expanded by the chain rule and the necessary arrangements are done, we can end up with

$$\lambda = \lim_{k \rightarrow \infty} \left[\frac{1}{k} \sum_{i=0}^{k-1} \ln |f'(x_i)| \right]. \quad (2.40)$$

2.8. THE LOGISTIC MAP

In 1976, Robert May published a review article in *Nature* which shows surprisingly that even simple and deterministic mathematical models can exhibit very complicated dynamical behaviors [12]. He analyzed a simple population growth model that has a recurrence relation as

$$x_{n+1} = rx_n(1 - x_n), \quad (2.41)$$

where x_n is the dimensionless measure of the population in the n 'th generation and r is the growth rate. The graph of the map is as follows:

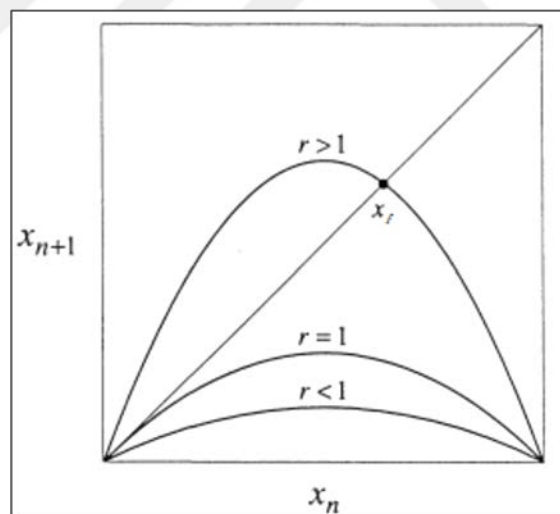


Figure 2.15. The Logistic map for different parameter r values.

One can also make the stability analysis by the cobweb diagram method for different parameter values as in Figure 2.16. It can be seen that while for some parameter values there is a converging behavior to the fixed point, there can be even chaotic behavior for some greater parameter values.

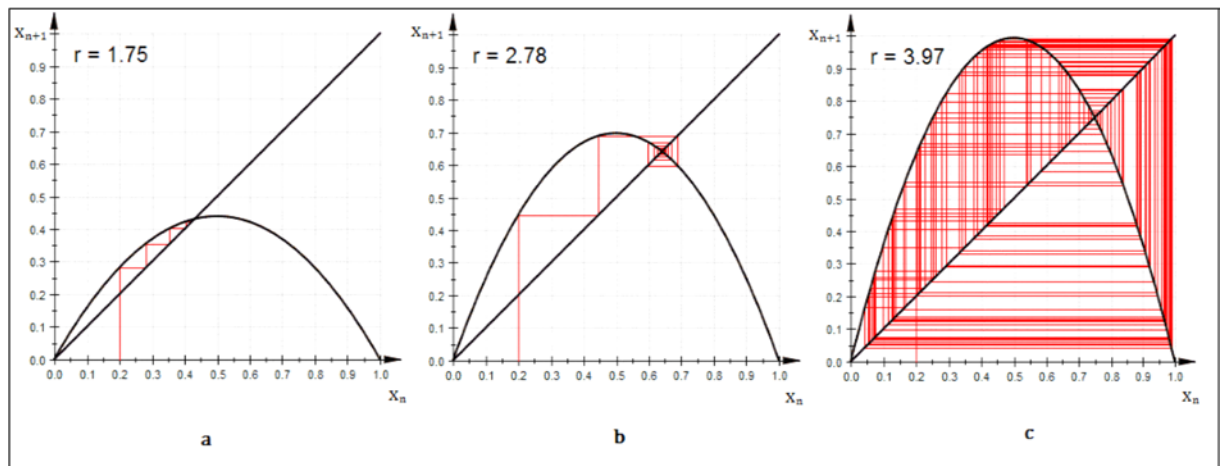


Figure 2.16. Graphical iterations and the cobweb constructions of the Logistic map for different parameter values [6].

Before going into the period doubling discussion, a kind of diagram, namely the bifurcation diagram can be introduced even though what bifurcation is will be stated in the next chapter.

Suppose a system that has a periodic orbit like in Figure 2.17.a and another system that has a period-II orbit as in Figure 2.17.b. If one observes one of the axes in the Poincaré section of Figure 2.17.a, sees just one value to which all the observation values are equal to. Similarly, for the system in Figure 2.17.b, one sees that all the observation values can have only two values; half of them take the one value and the other half take the other. If one draws a graph of a coordinate versus the parameter such that the transient points are eliminated and the system is allowed to gain its asymptotically stable behavior, and then only these discrete points are taken for the particular parameter values, the graph would be a bifurcation diagram. By changing the parameter, one can study the behavior of the system easily on the bifurcation diagram.

In the bifurcation diagram of the Logistic map (see Figure 2.18), the stable behavior of the system for particular parameter values can be seen. From starting point of the axis to the r

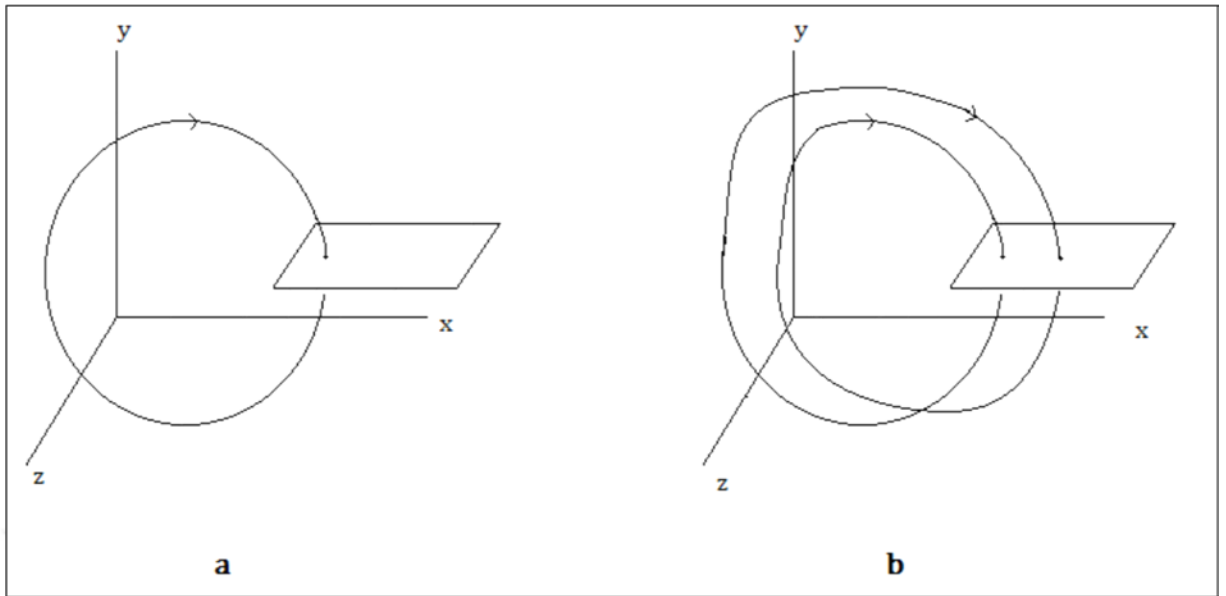


Figure 2.17. A period-I (a) and a period-II (b) orbits with Poincaré sections.

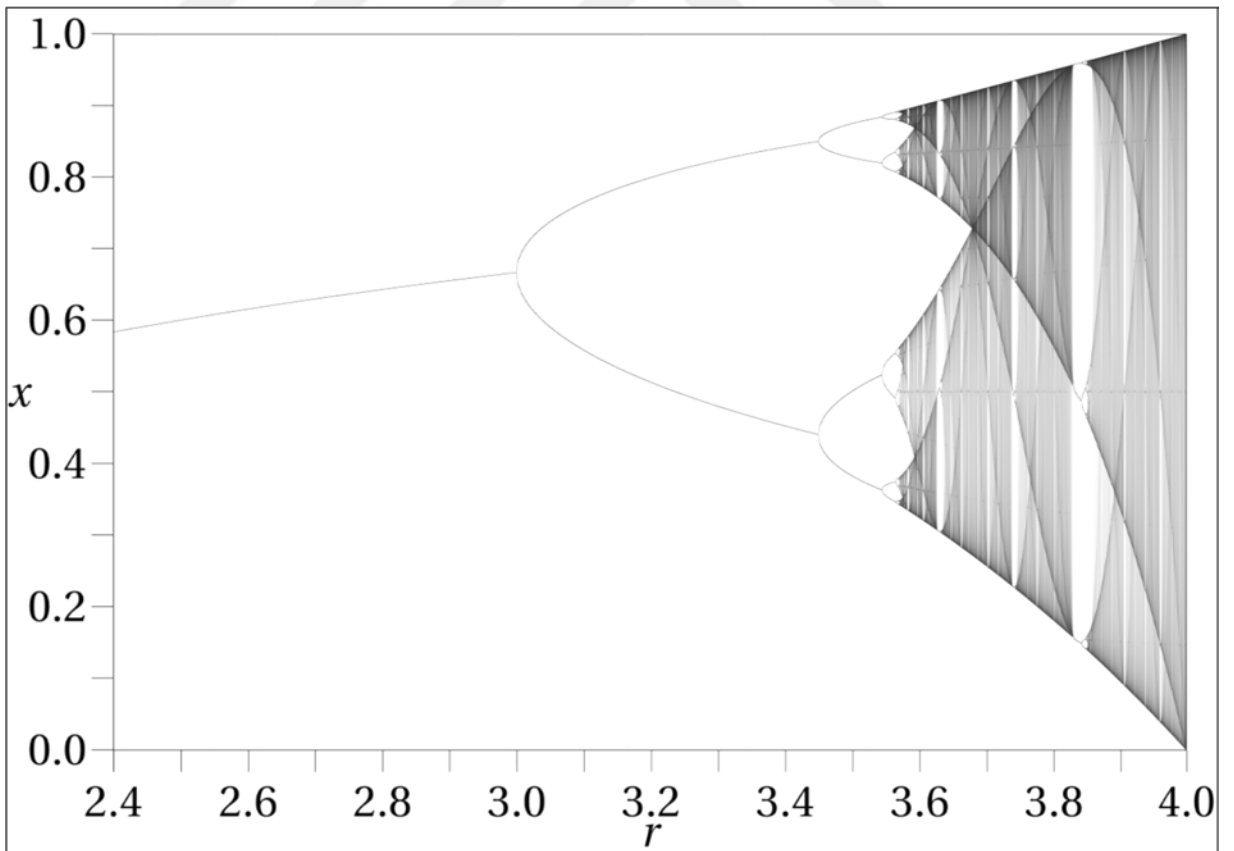


Figure 2.18. Bifurcation diagram of the Logistic map.

value approximately 3, the system behaves in a period-I mood; the plot splits into two and goes until somewhere between $r = 3.4$ and $r = 3.5$; and so forth. The plots split into two at some points, for example at $r = 3$. This phenomenon is known as period doubling.

2.9. BIFURCATIONS

A system and its behavior can be changed qualitatively under some circumstances depending on the parameters. Such changes in dynamics are called bifurcations, a term that was coined by Poincaré in 1885. A quantitative change in a system keeps the topological equivalence, but the qualitative change implies a break in the topological equivalency. Particularly saying, the stabilities of the fixed points or equilibria can be changed, or they can be formed and also can be destroyed. These kinds of changes alter the behavior of the system topologically.

There are several types of bifurcations like saddle-node, transcritical, pitchfork etc.

2.9.1. Period Doubling and Saddle-Node Bifurcations

The saddle-node bifurcation (also known as *tangent bifurcation*) is the basic mechanism for the fixed points to be created or be destroyed. As a parameter is changed, two fixed points can come closer to each other, collide, and can both be destroyed. The reverse can also happen.

Let's consider, for instance, the system

$$\dot{x} = r + x^2, \quad (2.42)$$

where r is a parameter. As can be seen in Figure 2.19, if r is less than zero, there are two fixed points. One of them is stable and the other one is unstable. As r goes to zero, two points move towards each other and they collide at the origin. The result is a half-stable fixed point. However, right after r passes zero, the fixed point annihilates. Thus, we say that a bifurcation occurred at $r = 0$, because the behavior of the system differs

topologically between the states when r is less than zero and greater than zero. The vector fields also changes as seen in the figure.

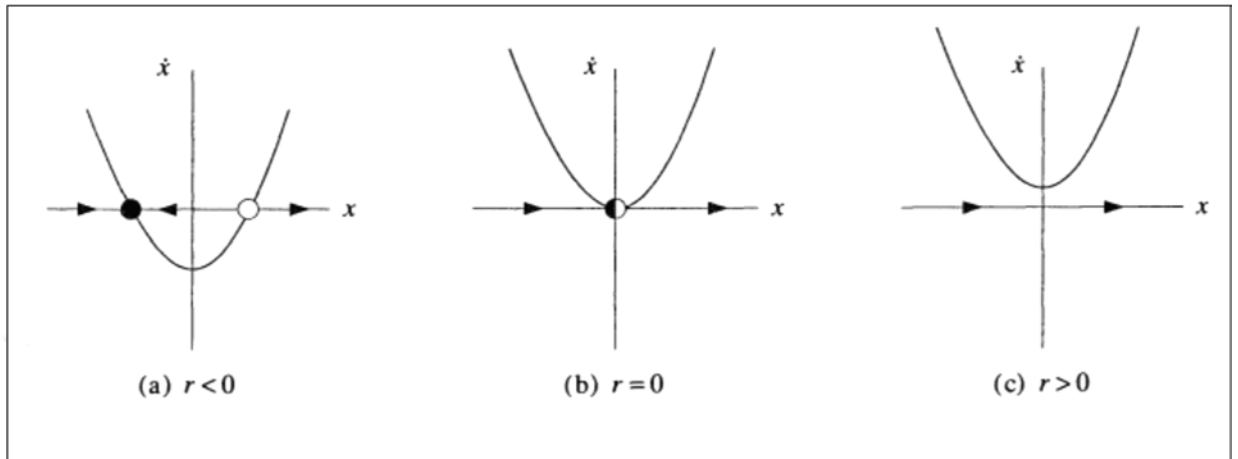


Figure 2.19. Two fixed points in (a), a half-stable fixed point in (b); and in (c), annihilation of the fixed point in (b) [5].

A special case of bifurcations is period doubling (also known as *flip bifurcation*). It is a kind of bifurcation that a pair of stable points comes into existence while the previously existing fixed point is destroyed. The destruction is only about the stability, not about the existence. It can be seen in Figure 2.18 easily. At around $r = 3$, a period doubling phenomenon occurs and the asymptotically stable behavior changes its behavior to a pair of, again, asymptotically stable new behaviors. Period doubling also occurs for each of the paths while r values are increased. To see the period doubling mathematically and clearly, let's begin with the Logistic equation. We first need to understand the creation and destruction mechanism of the fixed points.

$$x_{n+1} = rx_n(1 - x_n), \quad (2.43)$$

$$x_{nf} = rx_{nf}(1 - x_{nf}), \quad (2.44)$$

where x_{nf} is the fixed point of the n 'th generation. The fixed points can be found analytically from the equation, but there is an easy way to see them. In Figure 2.15, the

path for $r > 1$ have two intersection points with the 45° line: one is the origin and the other is x_f as it can be seen. One consideration is an important tool in such an analysis: If the slope of the tangent line at the intersection point is less than unity, the point is stable; if greater than unity, the point is not stable. That is why in Figure 2.15, for the corresponding line, the only fixed point is x_f and the origin is not. However, some conditions can be achieved while r is changing that there can occur two fixed points existing at the same time. For this, the slopes, that is, the derivatives can be investigated:

$$\frac{dx_{n+1}}{dx_n} = r - 2rx_n \quad (2.45)$$

For the two solutions of Eq. 2.44, Eq. 2.45 becomes

$$\frac{dx_{n+1}}{dx_n} = r \quad (2.46)$$

and

$$\frac{dx_{n+1}}{dx_n} = 2 - r. \quad (2.47)$$

For the values of r up to 1, the first one will be the stable point, and then up to 3, the second one will be the only stable point. After 3, that point also loses its stability, but not its existence. In this case, since the period-I orbit loses its stability, one can expect one of the two possibilities: The orbit can diverge to infinity or another orbit can become stable. To see this, one needs to do a check. To see if the period-II is stable, the Logistic equation for the second iteration is needed:

$$x_{n+2} = rx_{n+1}(1 - x_{n+1}) \quad (2.48.a)$$

$$= r^2x_n(1 - x_n)(1 - rx_n(1 - x_n)) \quad (2.48.b)$$

The fixed points are the fixed points of the first iteration that are no longer stable and two further points:

$$x_f = \frac{1+r \pm \sqrt{r^2-2r-3}}{2r} \quad (2.49)$$

The derivative:

$$\frac{dx_{n+2}}{dx_n} = \frac{dx_{n+2}}{dx_{n+1}} \frac{dx_{n+1}}{dx_n} \quad (2.50)$$

By the chain rule, things get easier. One can see that the total slope is less than unity; so, both points are stable. It can be seen also by the cobweb diagram:

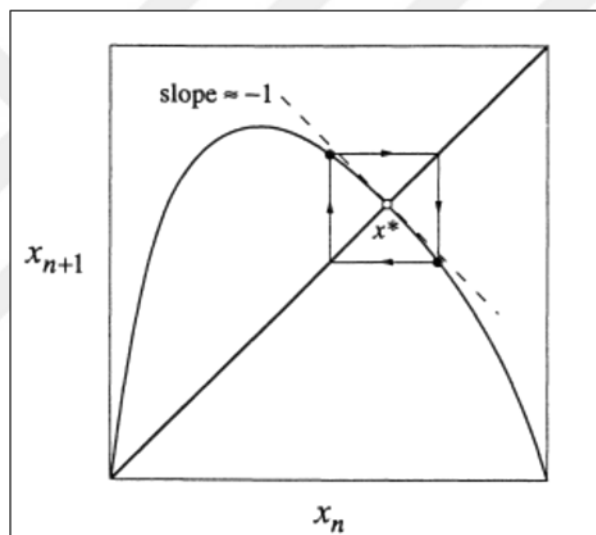


Figure 2.20. The cobweb diagram of a period-II orbit [5].

Any starting value will asymptotically converge to the shown cycle, the period-II cycle. Hence, by changing the parameter r , the stability of the period-I cycle is destroyed and a new cycle of period-II is created. The previous one actually does not lose its existence as we said before, but it loses its stability. It can be shown that the logistic map takes one of the fixed points to the other so that the period II attractor is created. The stability passes to the period-II cycle. This phenomenon is the period doubling. After some values of r , the period-II cycle also loses its stability and period-IV is created, and so forth as can be seen in the Figure 2.18. Robert May figured out that at approximately the value of r near 3.5,

things get very complicated and chaos occurs. That is, period-infinity orbit is created. In addition, while the period doubling can form chaos, period halving works for the order.

In a linear system, if the system becomes unstable, it collapses. Alternatively saying, the state goes to infinity. In a nonlinear system, system does not collapse, but it can go to another stable state. In a nonlinear system, instability frequently results in a bifurcation. Actually, there are different mechanisms that a system can lose its stability; two of them are period doubling bifurcation and saddle-node bifurcation.

2.9.2. Transcritical Bifurcation

Transcritical bifurcation is a special type of local bifurcation. It implies a mechanism for a bifurcation phenomenon which does not destroy the fixed point, but interchanges its stability. Thus, a fixed point keeps its existence for all values of the parameter. For instance, in the logistic equation, a fixed point exists at zero population and it is independent of growth rate. Nevertheless, the stability of the corresponding fixed point may change as the parameter varies.

The normal form of a transcritical bifurcation is

$$\dot{x} = rx - x^2. \quad (2.51)$$

The vector field for different parameter values can be seen in Figure 2.21. A fixed point sits at the origin and stays there as the parameter r changes. In Figure 2.21.a, there is an unstable fixed point at some value of x and a fixed point at $x = 0$ for $r < 0$. In Fig. 2.21.b, there is a half-stable fixed point which can stand only when $r = 0$. Finally, in Fig 2.21.c, when r becomes greater than zero, the fixed points changes and the origin becomes unstable while the other point gains stability.

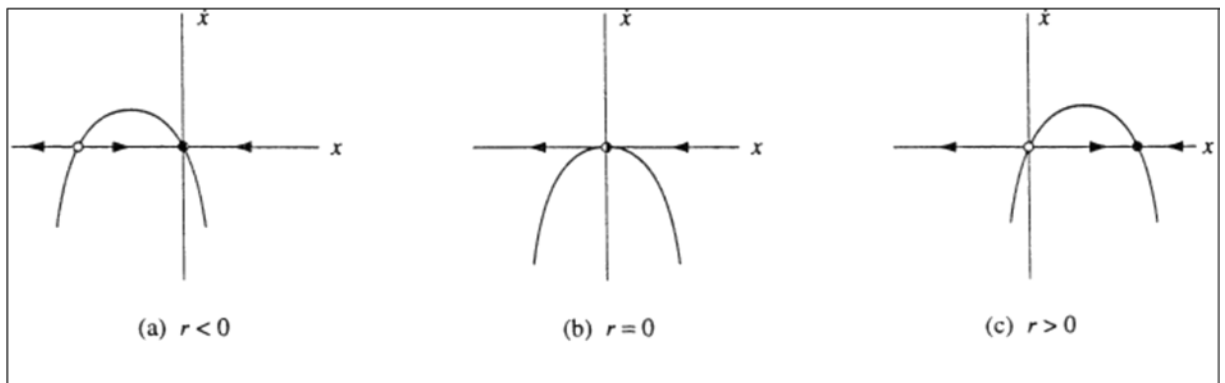


Figure 2.21. Two fixed points in (a) and (c), a half-stable fixed point in (b) [5].

2.9.3. Pitchfork Bifurcation

Pitchfork bifurcation is a special type of local bifurcation that is seen in systems having symmetry. It takes its name from its fork-like shape. It can be seen clearer in Figure 2.22. Since it is not possible to have such a bifurcation in normal logistic map, let's introduce another one:

$$x_{n+1} = (1 + r)x_n - x_n^3 \quad (2.52)$$

$$x_f = (1 + r)x_f - x_f^3 \quad (2.53)$$

$$x_{f0} = 0, \quad x_{f1} = \sqrt{r}, \quad x_{f2} = -\sqrt{r}$$

$$\frac{dx_{n+1}}{dx_n} = (1 + r) - 3x_n^2 \quad (2.54)$$

As can be seen, at $r = 0$, $\frac{dx_{n+1}}{dx_n} \Big|_{x_{f0}} = 1$. If it were -1, then period doubling would occur at that point, but here a pitchfork bifurcation phenomenon occurs which means that there becomes two independent period-1 orbits both of which are stable.

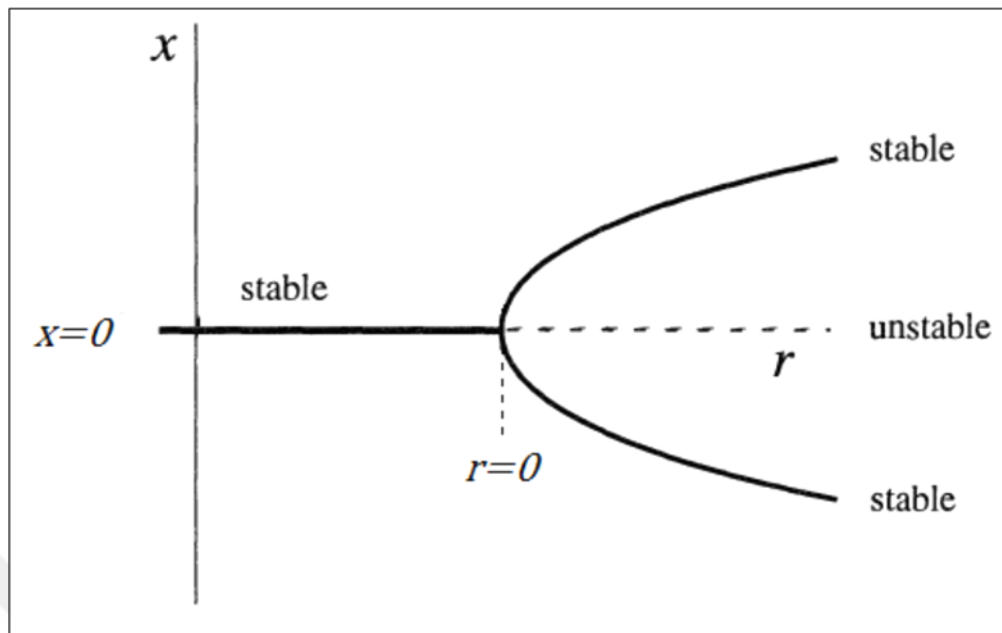


Figure 2.22. A bifurcation diagram with period doubling [5].

In period doubling bifurcation, a period-I orbit splits into a period-II orbit which implies that it is a flipping orbit. However, here in Figure 2.22 for example, if an initial point is given on the trajectory for $r > 0$, it stays on the same curve. If there was period doubling, it flips to the other curve and again flips to the previous, and keeps going flipping. Additionally, if an initial point near the trajectories is given, it is attracted by the stable trajectories. The trajectories are stable also for $r > 0$. It means that even the trajectory splits into two by period-doubling, the new trajectories are also stable.

2.10. FRACTALS

A fractal is, roughly speaking, the picture of chaos, the image of a dynamical system and the object of interest of the fractal geometry which is a discipline of mathematics first developed by Weierstrass in connection with continuous but not differentiable functions, but becoming important in last few decades. It attracted attention because of its possibilities of usefulness in applications of different disciplines of science and engineering.

As it is clear in its name, fractal geometry, it is geometry, and geometry deals with objects and the world or spaces they live in. For example, a point –which is a zero dimensional object- can live on a line -which is a one dimensional space in this case- or on a plane – which is a two dimensional space in this case; a plane –which is a two dimensional object- can live on a plane –which is a two dimensional space in this case- or in a three dimensional space. In the history of geometry or mathematics, people had been dealing with idealized objects like spheres, squares etc. These kinds of objects are ones that we cannot find in real life. However, for the sake of purpose, people idealized the objects that they wanted to make mathematical calculations on. This was so since Pythagoras and Euclid. In the last century, many developments in the theory of geometry were done. People began to think with not only Euclidean space but also curved space. Riemann and Minkowsky studied curved space; Einstein found an application of the thought of curved space in his theory about gravitation. However, the objects that we deal with remained as idealized.

While classical geometry deals with the idealized objects, a new type of geometry which deals with the real objects in life was born. One of the most famous examples to this kind of objects is the island on which Great Britain lives. The example was introduced by the father of fractals, Benoit Mandelbrot in a famous paper of his [13]. He explained his thoughts by using the question how long the coast of Britain is. He summarizes the answer by two sentences in the abstract: “Geographical curves are so involved in their detail that their lengths are often infinite or, rather, indefinable. However, many are statistically "self-similar," meaning that each portion can be considered a reduced-scale image of the whole”. Hereafter, he came up with the idea of fractional dimension.

His works on self-similarity and fractional dimension, actually, is the consolidation of all thoughts developed in the many years passed until his time. Maybe we can say that the first break in mathematical thought in the way to fractals was introduced by Leibniz in the idea of recursive self-similarity [14]. The content of the idea was of course crude, but the importance of the idea could not be ignored. Many developments in mathematical views had been made, but the last shot came with Mandelbrot that made him the father of fractal geometry.

The main difference coming up by fractal geometry is about differentiability of the objects in real world and the objects that are idealized. The objects in nature are continuous but not differentiable. However, people had been idealizing them to make calculations, and as a result, the objects become continuous and differentiable. Fractal geometry deals with the real objects that are continuous but not differentiable.

2.10.1. Dimension

To be able to analyze and understand the natural objects, we need a different formalism and somewhat different techniques other than the ones we use for idealized objects. In this manner, here comes the question of dimension.

Dimension of an object and dimension of embedding space are different things. While dimension of embedding space is about degrees of freedom, dimension of an object is about how it fills the space. For instance, let's we take a square that is lying on a two dimensional space or a plane. As in Figure 2.23, if we divide the space by smaller squares and count the number of small squares which fills the area of our square, we get the following relation between the number of boxes and the side length of the box:

$$N(d) = \left(\frac{1}{d}\right)^2, \quad (2.55)$$

where N is the number of small square boxes and d is the side length of the whole square.

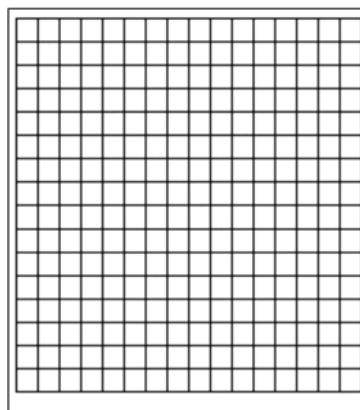


Figure 2.23. N small square boxes in one square.

We take the square of right-hand side of Eq. 2.55, because the dimension of the object was two. The equation for dimension can also be found by using Eq. 2.55. Since we know the dimension already, we will try to get 2. If we take the logarithm of both sides to get 2, the equation becomes

$$\ln N = 2 \ln \left(\frac{1}{d} \right) \quad (2.56)$$

$$\Rightarrow \text{Dimension} = \frac{\ln N(d)}{\ln \left(\frac{1}{d} \right)}. \quad (2.57)$$

Since in a square like in Fig. 2.23 can be filled exactly by finite number of smaller squares, the last equation holds for even for the example in Fig. 2.23. However, for other objects as a disk, we should take the limit of the right-hand side of Eq. 2.57, and again the result will be 2. Thus, the idea of dimension was expressed. For any object, the dimension is just the number that Eq. 2.57 converges to. For idealized objects, it becomes an integer, but it is not the case always, for instance, as we said, for the natural objects. So, for any natural object, we find the dimension that is not an integer. Objects that have fractional dimensions are fractals.

2.10.2. Cantor Set

Can we generate fractals? Yes, we can generate fractals by some iterative processes. A much known discovery about generating fractals is the cantor set. It was discovered by H. J. Steven Smith in 1874 [15], and introduced by Georg Cantor in 1883 [16]. Cantor set is a fractal with an embedding space of one dimension, that is, a line.

Let's assume that we cut and delete the middle third of the closed interval $S_0 = [0,1]$ as in Fig. 2.24. If we resume by doing the same thing to the new intervals separately, we obtain the Cantor set at the limit as going to infinity. The resulting set includes infinite many pieces that have different gaps between each other.

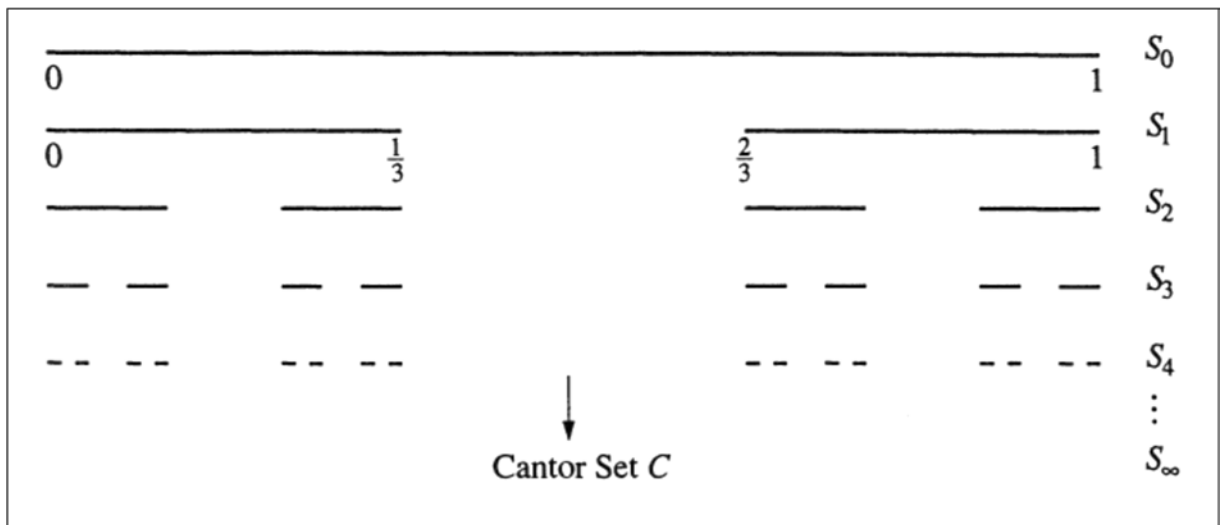


Figure 2.24. The Cantor Set and the iterative evolution to it [5].

If we want to look at the set if it is a fractal or not, we can calculate the dimension: For S_1 , $N = 2$ and $d = \frac{1}{3}$, and so the dimension for the first step is

$$D = \lim_{d \rightarrow 0} \left(\frac{\ln N(d)}{\ln \left(\frac{1}{d} \right)} \right) = \frac{\ln 2}{\ln 3}. \quad (2.58)$$

Similarly, if we do the same procedure for other steps, we conclude with the fact that the dimension D is the same for all steps. Thus, the dimension of the set C is the same with previous steps which is a fractional number.

Another important feature of the set is that it has a self-similarity. That is, it includes copies of itself at any scale. Cantor Set is a famous example of fractals.

2.10.3. Chaos Game

We mentioned that a chaotic behavior is actually a deterministic one. To see this in context of fractals, *chaos game* –was coined by Michael Barnsley– is a good example [17]. Actually, by the method, we can generate an attractor of an iterated function system (IFS). We can create a sequence of points, which will be a fractal, by an iterative process. The

remarkable point is that we use randomness in the process, but we get deterministic fractals at the end. To see it more clearly, we can look at a known example: Sierpinsky gasket.

Suppose three points $P_1 = (a_1, b_1)$, $P_2 = (a_2, b_2)$ and $P_3 = (a_3, b_3)$ on a coordinate system with x – and y – axes as located in Fig. 2.25, and a current *game point* $z_k = (x_k, y_k)$ somewhere arbitrary on the plane. We randomly get one of the three points which are at the corners of the triangle, say P_2 . We generate the next game point z_{k+1} which will locate at the midpoint between z_k and P_2 : $z_{k+1} = f_n(z_k) = (x_{k+1}, y_{k+1})$, where f is our affine map, n is the random event, $x_{k+1} = \frac{1}{2}x_k + \frac{1}{2}a_n$ and $y_{k+1} = \frac{1}{2}y_k + \frac{1}{2}b_n$. Note that the probabilities of the random events are equal.

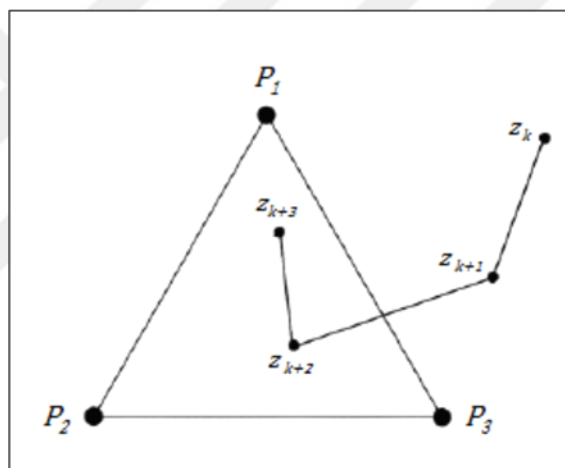


Figure 2.25. The Chaos game board and the first three steps that are connected by line segments.

This is the first step of the game, and the other steps will come similarly. If we keep iterating, the resulting shape of the generating dots, the game points, will begin to form a specific fractal, namely Sierpinsky gasket as shown in Fig. 2.26. Here we conclude with an interesting thing: By a random process we can create a deterministic shape. That is, although we cannot predict where the next point will come up in the game, the resulting shape that the collection of all these points form is predictable.

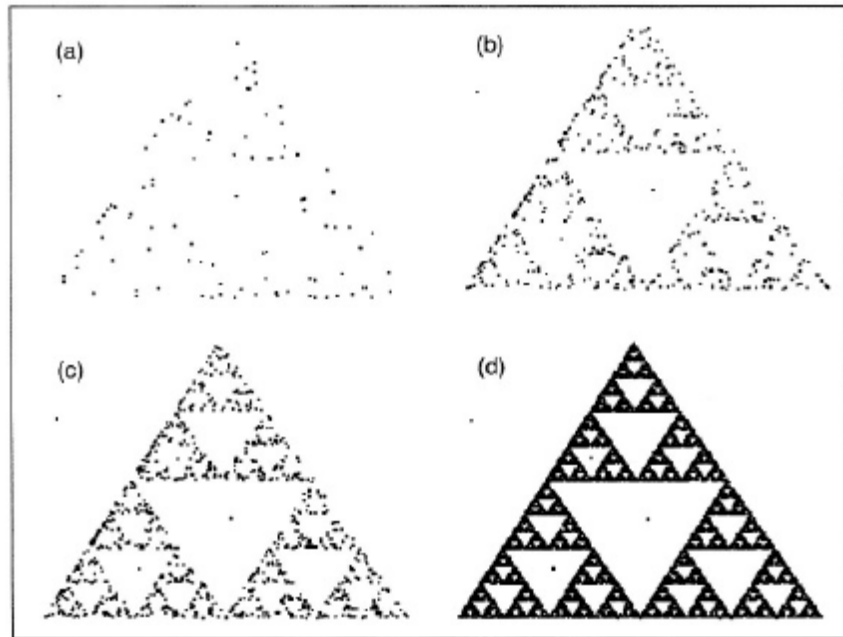


Figure 2.26. The chaos game after 100 steps (a), 500 steps (b), 1000 steps (c) and 10,000 steps (d) [16].

3. DIFFUSION IN CONDENSED MATTER

Diffusion in condensed matter systems is an important topic in physics. The subject has an important role in the kinetics of microscopic changes which happens in processes of metals, semiconductors, ceramics, thin glasses etc.

From a phenomenological point of view, diffusion is the net movement of a substance from a region with higher concentration to one with lower concentration. The substance can be atoms, ions, molecules, electrons, people, money or even ideas and any item that can diffuse.

3.1. FICK'S LAWS OF DIFFUSION

Fick's equations are known as the equations that describe diffusion. The diffusion of particles through condensed matter can also be described by Fick's equations. He stated his first law in 1855 [18] before Maxwell and Boltzmann had introduced their kinetic theory of gases, and hence before the random walk picture of the diffusion process was established [19]. Thus, we can say that Fick set his theory from a phenomenological point of view. His theory goes with an analogy with Fourier's theory of heat flow (1822). The heat current density is proportional to the gradient of temperature (for 1-D):

$$j_H = -\lambda \frac{\partial T}{\partial x}, \quad (3.1)$$

where j_H is the heat current density, T is the temperature, x is the position and λ is the conductivity of the material. In addition, a similar relation can be given as Ohm's law for electrical current (1827):

$$j_e = -\sigma \frac{\partial \varphi}{\partial x}, \quad (3.2)$$

where j_e is the electric current density, φ is the electrostatic potential and σ is the conductivity of the material. As in these equations (Eqs. 3.1, 3.2), the relation between the diffusive flux j to the concentration $\phi(x)$ can be given as

$$j = -D \frac{\partial \phi}{\partial x}, \quad (3.3)$$

where D is the diffusion coefficient or the diffusivity. Eq. 3.3 is known as Fick's first law. Fick's second law describes the change in concentration with time in diffusion phenomena. Combining Fick's first law with the continuity equation gives Fick's second law.

The continuity equation is given as

$$\frac{\partial \phi(x,t)}{\partial t} = -\frac{\partial j(x)}{\partial x}, \quad (3.4)$$

and combining this with Eq. 3.3 gives

$$\frac{\partial \phi}{\partial t} = D \frac{\partial^2 \phi}{\partial x^2}. \quad (3.5)$$

This is known as Fick's second law. The solution subject to an initial condition of a point source is given by [19]

$$\phi(x, t) = \frac{1}{\sqrt{4\pi Dt}} e^{-\frac{x^2}{4Dt}}. \quad (3.6)$$

3.2. COLLISION MODEL AND BROWNIAN DIFFUSION

Another way of introducing the diffusion phenomenon is the collision model of particles. Diffusion can be considered as a consequence of the random walk of the *diffusing* particles. Random walk of small particles, small pollen grains, which are suspended in a fluid (water) was observed by the Scottish botanist Brown in 1827 [20]. Although Brown could not understand the nature beyond the motion of the grains, we know that it is caused by the collisions of the quick particles in the fluid. Some attempts for explanation of Brownian motion and developments of these explanations were done, and finally in 1905, Einstein gave a definitive explanation of the Brownian motion by unifying the continuum formulation given by Fick and the stochastic theory based on the collision model [21].

Einstein's explanations were based on two assumptions: the extremely frequent collisions of the particles in the fluid and the atoms or molecules of the fluid; and the motion can only be described by probabilistic models, because the motion is very complicated.

He assumed that the number of particles is conserved and expanded the variation of the particle concentration change in a Taylor series:

$$\begin{aligned}\phi(x, t + \tau) &= \phi(x, t) + \tau \frac{\partial \phi(x)}{\partial t}, \\ &= \int_{-\infty}^{\infty} \phi(x + \chi, t + \tau) p(\chi) d\chi \\ &= \phi(x, t) \int_{-\infty}^{\infty} p(\chi) d\chi + \frac{\partial \phi}{\partial x} \int_{-\infty}^{\infty} \chi p(\chi) d\chi + \frac{\partial^2 \phi}{\partial x^2} \int_{-\infty}^{\infty} \frac{\chi^2}{2} p(\chi) d\chi + \dots,\end{aligned}\tag{3.7}$$

where the first integral is 1 from the definition of probability, and second one with other even terms is 0 from the symmetry; p is some probability density function. Thus,

$$\frac{\partial \phi}{\partial t} = \frac{\partial^2 \phi}{\partial x^2} \int_{-\infty}^{\infty} \frac{\chi^2}{2\tau} p(\chi) d\chi + \dots,\tag{3.8}$$

where the integral term is interpreted as mass diffusivity, D . The density of particles ϕ that manifest Brownian motion at point x and at time t satisfies Eq. 3.5; and the solution is given by Eq. 3.6. By this expression (Eq. 3.6), we can find the moments directly. However, the first one is zero, since the particle tends to move right and left equally. The next moment does not vanish and can be found by the mean squared displacement as a linear function of the time:

$$\langle x^2 \rangle = \int_{-\infty}^{\infty} x^2 \phi(x, t) dx = 2Dt\tag{3.9}$$

3.3. ANOMALOUS DIFFUSION

It can be seen that Eq. 3.6, the solution to Fick's second law, is a Gaussian probability density function. By the Gaussian diffusion equation, we can describe many diffusion processes [21]. However, there are also other diffusion processes that we cannot describe

by the Gaussian diffusion equation. Such processes are called as anomalous diffusions and they are nonlinearly related to time. In the case of anomalous diffusion, we can think of a diffusion process goes on under different rules of *walking*, instead of typical random walking. It can be described by a different probability density function other than Eq. 3.6, which will depend in this case nonlinearly to time as follows:

$$p(x, t) = \frac{1}{t^\delta} F\left(\frac{x}{t^\delta}\right), \quad (3.10)$$

where δ is the scaling constant and F is usually some exponential function. While the mean squared displacement of a particle is a linear function of time for normal diffusion, as in Eq. 3.9, it is a nonlinear function of time for anomalous diffusion:

$$\langle x^2 \rangle = \int_{-\infty}^{\infty} x^2 p(x, t) dx \sim Dt^\alpha, \quad (3.11)$$

where α is a constant and it is given as some times δ according to the conditions of the process.

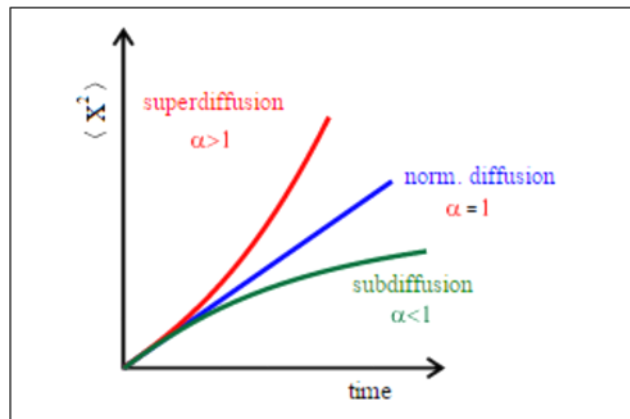


Figure 3.1. Mean squared displacement vs. time graph for different types of anomalous diffusion.

If $\alpha = 1$, the process is typical diffusion; if $\alpha > 1$, the process is called super diffusion; if $\alpha < 1$, the process is called sub diffusion. These three types of diffusion can be seen in Figure 3.1.

4. NONEXTENSIVE STATISTICAL MECHANICS

Statistics and dynamics are two separate and basic elements of the physics near thermodynamic equilibrium. Under the condition of thermodynamic equilibrium, Boltzmann-Gibbs (BG) statistical mechanics gives useful results as the nature manifests itself as a Gaussian. Actually, a master equation such as the Boltzmann transport equation can be written and under suitable approximations, the laws of thermodynamics near equilibrium can be derived, however this is not necessary. However, under the conditions far from the equilibrium, for example for most of the so-called complex systems, this does not work and hence statistics and dynamics need to be unified. Constantino Tsallis was the one who first achieved this [22].

His main attempt can be summarized in one sentence: He wanted to connect in theory our understanding in the sense of statistics of the macroscopic world and the microscopic world. Near equilibrium where BG statistics works, we do not need to know the microscopic states of the subsystems of a system and able to calculate the entropy of the composed system macroscopically. However, for complex systems which have common characteristics as long-range correlations, multifractality and non-Gaussian distributions, and composability of the BG entropy disappears and hence becomes unuseful. What Tsallis has done is to enlarge the applicability domain of the frame of Boltzmann and Gibbs's theory by extending the mathematical form of its entropy [23]. Generalizing the mathematical form of the entropy has connected the microscopic world with its macroscopic appearance. Nonextensive statistical mechanics has found many applications in different disciplines including physics, chemistry, biology, mathematics, economics, geography, linguistics etc. [24, 25].

4.1. BOLTZMANN-GIBBS STATISTICAL MECHANICS

Boltzmann first proposed his entropic formula in 1870s [26, 27, 28] and Gibbs then developed it for more general systems [29]. If the appropriate variables are continuous, the BG entropy is given in the form

$$S_{BG} = -k \int dx p(x) \ln(\sigma p(x)) \quad (4.1)$$

with

$$\int dx p(x) = 1, \quad (4.2)$$

where k is some conventional positive constant and $\frac{x}{\sigma} \in \mathbb{R}^D, D \geq 1$ being the dimension of Gibbs Γ phase-space for classical Hamiltonian systems; $\frac{x}{\sigma}$ is a dimensionless quantity, since they carry the same physical units. For discrete states, the BG entropy takes the form

$$S_{BG} = -k \sum_{i=1}^W p_i \ln(p_i) \quad (4.3)$$

with

$$\sum_{i=1}^W p_i = 1, \quad (4.4)$$

where W is the number of discrete states. For equal probabilities, that is, $p_i = \frac{1}{W}$ for every i , Eq. 4.3 becomes

$$S_{BG} = k \ln(W). \quad (4.5)$$

There are various important properties of the BG entropy such as non-negativity, expansibility, additivity, concavity, Lesche-stability or experimental robustness, composability etc. [23]. It will be useful to give here the property of additivity, because this is one of the properties that has the basic importance in relation with the concept of extensivity and nonextensivity.

If A and B are two probabilistically independent subsystems with large number of states W_A and W_B respectively, and the joint probabilities factorize as $p_{ij}^{A+B} = p_i^A p_j^B$ for every (i, j) , S_{BG} is said to be additive [30]. That is,

$$S_{BG}(A + B) = S_{BG}(A) + S_{BG}(B), \quad (4.6)$$

where

$$S_{BG}(A + B) = -k \sum_{i=1}^{W_A} \sum_{j=1}^{W_B} p_{ij}^{A+B} \ln(p_{ij}^{A+B}) \quad (4.7)$$

with $W = W_A W_B$;

$$S_{BG}(A) = -k \sum_{i=1}^{W_A} p_i^A \ln(p_i^A) \quad (4.8)$$

and

$$S_{BG}(B) = -k \sum_{j=1}^{W_B} p_j^B \ln(p_j^B). \quad (4.9)$$

4.2. GENERALIZATION OF THE BOLTZMANN-GIBBS STATISTICAL MECHANICS

Since we cannot generalize any physical theory in a logical-deductive way, one of the possible figurative expressions for the generalization of the BG entropy can be given as Tsallis did [23]:

Let's take the following simple three differential equations, their solutions and the inverse functions of the solutions, respectively:

$$\frac{dy}{dx} = 0 \quad (y(0) = 1), y = 1, x = 1; \quad (4.10)$$

$$\frac{dy}{dx} = 1 \quad (y(0) = 1), y = 1 + x, y = x - 1; \quad (4.11)$$

$$\frac{dy}{dx} = y \quad (y(0) = 1), y = e^x, y = \ln(x). \quad (4.12)$$

To unify these three equations, we can consider

$$\frac{dy}{dx} = a + by \quad (y(0) = 1), \quad (4.13)$$

where a and b are some parameters. Changing the parameters gives us the opportunity of reobtain the corresponding equations. On the other hand, we can also unify the corresponding equations with one parameter. In this case, we lose the linearity. To see this, let's consider

$$\frac{dy}{dx} = y^q (y(0) = 1; q \in \mathbb{R}), \quad (4.14)$$

whose solution is

$$y = [1 + (1 - q)x]^{1/(1-q)} \equiv e_q^x \quad (e_1^x = e^x) \quad (4.15)$$

and the inverse function of the last equation is

$$y = \frac{x^{1-q}-1}{1-q} \equiv \ln_q(x) (x > 0; \ln_1(x) = \ln(x)). \quad (4.16)$$

$\ln_q(x)$ satisfies the following property:

$$\ln_q(x_A x_B) = \ln_q(x_A) + \ln_q(x_B) + (1 - q) (\ln_q(x_A)) (\ln_q(x_B)) \quad (4.17)$$

The q -deformed special presentations of Eqs. 4.15 and 4.16 are called as the q -exponential and the q -logarithm as Tsallis first introduced in 1994 [31]. It can be easily seen that Eq. 4.14 recovers Eqs. 4.10, 4.11 and 4.12 respectively for the $q \rightarrow -\infty$, $q = 0$ and $q = 1$ cases.

Through the above metaphor, we can conclude with the generalization of the BG entropy (Eq. 4.5):

$$S_q = k \ln_q(W). \quad (4.18)$$

Note that S_q becomes S_{BG} for $q = 1$. Since Eq. 4.3 can be rewritten as

$$S_{BG} = k \langle \ln(1/p_i) \rangle, \quad (4.19)$$

we can also rewrite Eq. 4.18 as

$$S_q = k \langle \ln_q(1/p_i) \rangle, \quad (4.20)$$

and using Eq. 4.16 yields finally the possible basis for generalization of BG statistical mechanics:

$$S_q = k \frac{1 - \sum_{i=1}^W p_i^q}{q-1}. \quad (4.21)$$

S_q preserves the various properties of the BG entropy such as non-negativity, expansibility, concavity, Lesche-stability or experimental robustness, composability etc. [23]. However, additivity is the key point that also pushed Tsallis to search a new or better entropic form. In this case, nonadditivity is the main property of S_q .

4.3. GENERALIZED DISTRIBUTIONS AND THE q -GAUSSIAN

Generalized distributions or Tsallis distributions or q -distributions are the probability distributions derived by maximizing the Tsallis entropy under appropriate constraints. The generalized distributions can be obtained by following a number of different procedures. A very simple one is just replacing the exponential function of the original distribution by a q -exponential function. For instance, when the corresponding method is applied in standard exponential, Gaussian and Weibull distributions, the q -ones of the distributions are obtained; namely q -exponential, q -Gaussian and q -Weibull respectively [32]. Similarly, other q -distributions are also obtained.

q -Gaussian distribution is one of the special cases arises from the maximization of S_q by using the appropriate constraints. The q -Gaussian distribution is defined by the PDF

$$p_{qg}(x) = p_0 \left[1 - (1 - q) \left(\frac{x}{x_0} \right)^2 \right]^{1/(1-q)}, \quad (4.22)$$

for

$$\left[1 - (1 - q) \left(\frac{x}{x_0} \right)^2 \right] \geq 0 \quad (4.23)$$

and otherwise $p_{qg}(x) = 0$. The PDF is normalized when

$$p_0 = \left(\frac{2}{x_0}\right) \frac{\sqrt{\frac{q-1}{\pi}} \Gamma\left(\frac{1}{q-1}\right)}{\Gamma\left(\frac{3-q}{2(q-1)}\right)}. \quad (4.24)$$

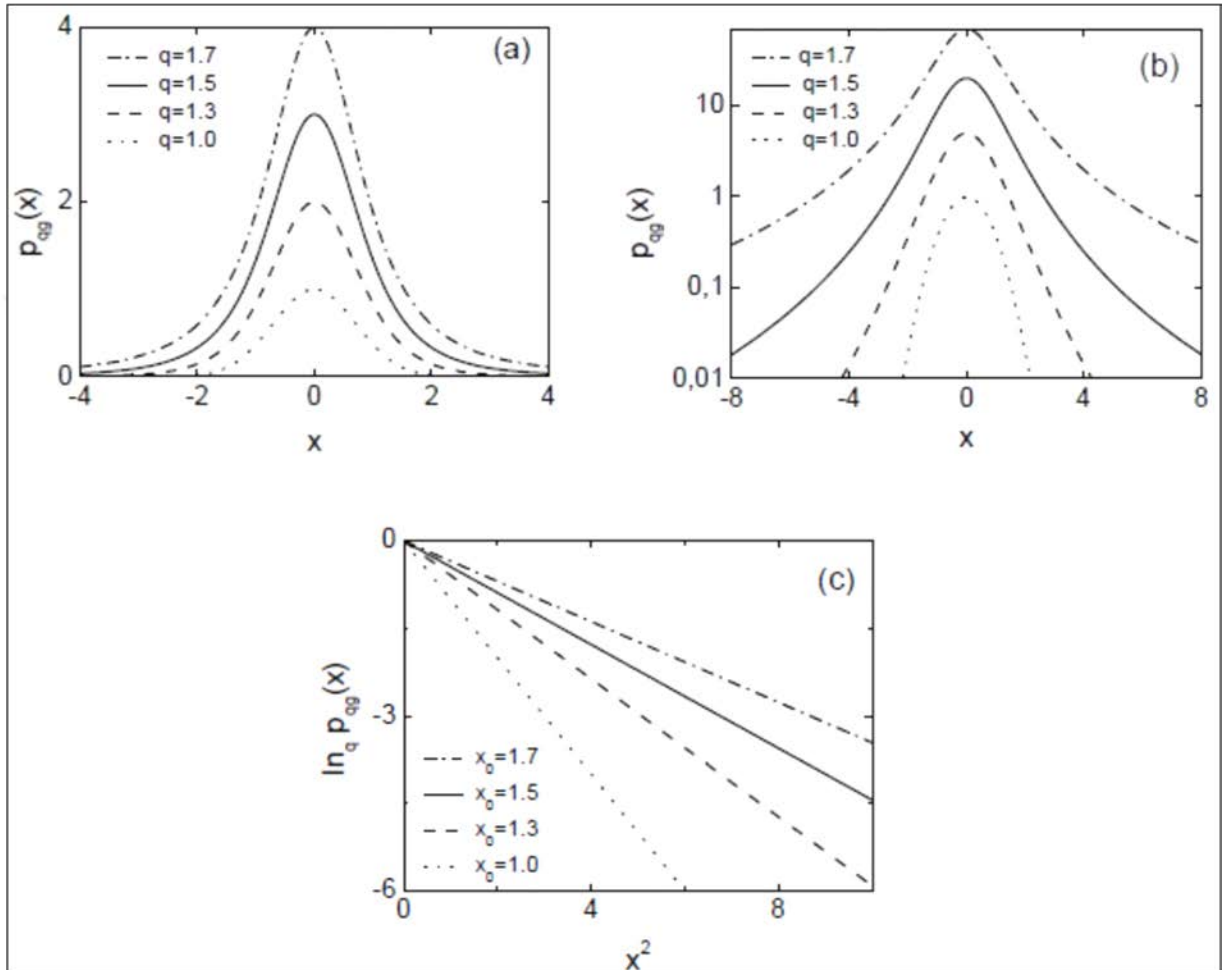


Figure 4.1. q -Gaussian distribution. (a) Plot of $p_{qg}(x)$ vs. x , with $p_0 = x_0 = 1$, for different values of q . (b) The same curves of (a) for mono-log scale. (c) $\ln_q(p_{qg}(x))$ vs. x^2 for $p_0 = 1$ and different values of x_0 . [33].

For the limit case where $q \rightarrow 1$, Eq. 4.24 becomes the standard Gaussian distribution. So, $q \neq 1$ implies the regime where Gaussian statistics does not work. If $q > 1$, $p_{qg}(x)$ becomes

$$p_{qg}(|x|) \sim |x|^{2/(1-q)} \quad (4.25)$$

as shown in Figures 4.1.a and 4.1.b.

q -logarithm of $p_{qg}(x)$ is

$$\ln_q(p_{qg}(x)) = \ln_q(p_0) - [1 + (1 - q)\ln_q(p_0)]\left(\frac{x}{x_0}\right)^2 \quad (4.26)$$

and Figure 4.1.c shows $\ln_q(p_{qg}(x))$ vs. x^2 for different values of x_0 .

q -Gaussian distributions find various application areas such as finance [34,35], genetics [36], mathematics [37], meteorology [38], earthquakes [39] etc.

5. ANALYSIS OF CHAOTIC SYSTEM BEHAVIORS

Many scientists from various fields have been influenced by the thought of deterministic chaos or chaos theory. Chaos theory gives powerful explanations to the behaviors of inherent systems which do not seem to be naturally stochastic. By nonlinear time series analysis we can make contact between the real world and chaos theory.

We can interpret the regular structure of a data set by linear methods and we ascribe the irregular behavior of the system as random external inputs. However, in many cases, that is, in real cases that we take data describing the behavior of a natural system, this is not the case. Random input is not the only source of irregularity. Nonlinear systems can yield deterministic but irregular data which require an approach other than that of linear methods. Nonlinear time series analysis is the way for quantification and analysis of the chaotic system behaviors.

A time series is a sequence of collected data obtained by repeated measurements over time. Irregularly collected data is not a time series. We use time series analysis to extract meaningful statistics or some characteristics of the corresponding data. For instance, as in our study, we can use time series analysis to understand the behavior of a thin-film for making predictions about its behavior under certain conditions.

We can find three components in an observed time series. The trend: it implies long term direction; the seasonal: it implies systematic and/or calendar related flow; the irregular: it implies unsystematic, short term surges. The last one, irregular fluctuations, may not be always unsystematic. If there is a chaotic system behavior, although the measurement of an observation seem like it has an irregularity, there is not. The behavior of the system will be completely deterministic. When an orbit $x(t)$ evaluates in a nonlinear sense and under the rules of differential equations

$$\frac{dx(t)}{dt} = f(x(t)) \quad (5.1)$$

or discrete time maps

$$x(t + 1) = f(x(t)), \quad (5.2)$$

chaos phenomenon can occur [40, 41, 42]. While in systems as described by Eq. 5.1 degrees of freedom is determined by the number of first order autonomous ordinary differential equations required, in discrete time systems as described by Eq. 5.2 it is the same as the number of components of $x(t)$ [43]. As discussed above, some aspects of chaos will show up themselves by traces of complex time with continuous Fourier spectra, nonperiodic trajectories in the state space, and great sensitivity to little changes in the orbit. With linear methods like Fourier transform, chaotic behaviors cannot be analyzed. Actually, chaos appears like noise in the data. To get meaningful information from scalar time series, we need some nonlinear methods.

5.1. PHASE SPACE RECONSTRUCTION

Since in study of deterministic systems phase space has a significant importance, it brings together the question that the thing we observe is not a phase space object, but a time series only. Thus, we need to convert the observation, which is just a sequence of scalar measurements, into state vectors. Phase space reconstruction is the solution to this problem. It can be handled by delay methods.

A chaotic time series which is a scalar observation is usually embedded into a delay reconstructed phase space by the embedding theorem of Takens [44, 45]. The theorem states the following: Given a dynamical system as in Eq. 5.1 in a phase space $\Gamma \in \mathbb{R}^d$, a measurement function $h: \mathbb{R}^d \rightarrow \mathbb{R}$, and a sampling interval Δt . Assume that the system f has a strange attractor with box-counting dimension d_f . Denote the scalar measurements obtained through the sampling by $s_n = h(x(t = n))$. Consider the delay embedding space spanned by delay vectors $\vec{s}_n = (s_n, s_{n-\tau}, \dots, s_{n-(m-1)\tau})$. The attractor can be embedded in d_e -dimensional space if $d_e > 2d_f$. When d_e is chosen to be greater than $2d_f$, which can be fractional, overlaps can be removed and the orbit would be unambiguous.

In conclusion, we can say that the phase space reconstruction method supplies us the opportunity by which, beginning with a set of scalar data $s(t_0 + n\tau_s) = s(n)$ and using $s(n)$ and its time delays, we can get vectors

$$\vec{y}(n) = [s(n), s(n + \tau), s(n + 2\tau), \dots, s(n + (d_e - 1)\tau)] \quad (5.3)$$

in d_e -dimensional space which do not falsely cross the orbits $\vec{y}(n)$. They do not false cross, because they are projected from a higher dimensional space. In addition, we underlined a special criterion $d_e > 2d_f$ for the number of elements in $\vec{y}(n)$.

Phase space reconstruction method conserves the information of the invariants of the original system, so we can investigate the invariants as they are in the original space. To make the things more manageable, we need to determine an optimal dimension and a suitable time lag.

5.2. CHOOSING TIME DELAYS

To reconstruct a phase space, choosing suitable time lags is an important issue as we mentioned above. For instance, if we choose a time delay larger than what is needed, $s(n)$ and $s(n + \tau)$ could be completely independent in a statistical sense. On the other hand, if we choose the delay too short, they could not be independent enough, and this causes a loss of some of information that we need about the original system.

The typical choice of threat to the problem is based on the generation of information. That is, the choice of time delay is made basing on the generation of information. Since stable linear systems do not produce information [43], we need to focus on a property which is not shared both with linear and nonlinear systems, but is shared with only nonlinear ones.

5.2.1. Auto-correlation Function

Auto-correlation is, simply, the cross-correlation of a signal with itself. It gives the similarities between the observed data in terms of time delay. By auto-correlation function, we can measure the correlation of a signal with itself shifted by a time lag; the auto-correlation function is defined as follows:

$$A(t) = \frac{\frac{1}{N} \sum_{m=1}^N (S(m+t) - \bar{S})(S(m) - \bar{S})}{\frac{1}{N} \sum_{m=1}^N (S(m) - \bar{S})^2}, \quad (5.4)$$

where \bar{S} is defined as

$$\bar{S} = \frac{1}{N} \sum_{m=1}^N S(m). \quad (5.5)$$

We can find the periodicity in a signal by the function and identify the effect of noise on the signal.

If there is no noise, the auto-correlation function oscillates with constant amplitude and the periods of the function and the signal would fit each other. If there is noise, the envelope of the auto-correlation function decreases; and by looking at how fast it decreases, we can quantify the effect of noise.

5.2.2. Mutual Information

Mutual information of two variables implies the mutual dependence of them; that is, it tells about how much we can get information about one of the variables by looking the other. While the linear dependence can be measured by the auto-correlation, a more general dependence can be received by the mutual information. Hence, the mutual information is a preferable measure of the transition from small t to large t with nonlinear systems.

The mutual information of two discrete random variables is defined as follows:

$$I(X; Y) = - \sum_{x \in X} \sum_{y \in Y} p(x, y) \log \left(\frac{p(x, y)}{p(x)p(y)} \right), \quad (5.6)$$

where X and Y are the random variables, $p(x, y)$ is the joint probability distribution function of X and Y , and $p(x)$ and $p(y)$ are the marginal probability distribution functions of X and Y respectively. The numerical scale of the measure of the information, $I(X; Y)$, is determined by the base of the logarithm in Eq. 5.6: If the base of logarithm is 2, then we call the scale of the number we get by $I(X; Y)$ as “bit” (binary digit); if the base is e , the scale would be “nat” (natural unit) [46].

5.3. CHOOSING THE DIMENSION

While the observed orbits of the attractor are projected to a lower dimensional space, there occurs some overlaps and hence a loss of information. To avoid this, we need to find an integer dimension by which we can get the necessary number of coordinates. In that sense, we need to look at the system to figure out the condition that causes these overlaps. That is, thinking the dimension as a parameter, for what dimension value we get rid of the overlaps. We better try to find the minimum value to minimize the algebraic effort. This minimum dimension which is an integer is called the embedding dimension, d_e . It is worth to emphasize one thing: It is not necessary to be the same that the embedding dimensions obtained from different observations of two quantities of the same system.

As we mentioned above, the sufficient –not necessary- condition to avoid the overlaps is $d_e > 2d_f$, where d_f is the dimension of the attractor defined by the orbits. Since d_e represents not the necessary but only the sufficient condition, this means that we can select one of the many possible dimensions.

5.3.1. False Nearest Neighborhood Method

We want to find a criterion for the embedding dimension which can cause to unfold the attractor. We prefer the dimension to be the minimum, since it is easier to handle. The false nearest neighbors method is one of the well-known methods for the job.

The method recommends beginning with thinking on the data vectors of the reconstructed space and the nearest neighbor in phase space of these vectors:

$$\vec{y}(n) = [s(n), s(n + \tau), \dots, s(n + (d_e - 1)\tau)] \quad (5.7)$$

$$\vec{y}_{NN}(n) = [s_{NN}(n), s_{NN}(n + \tau), \dots, s_{NN}(n + (d_e - 1)\tau)] \quad (5.8)$$

Eq. 5.7 gives the data vectors, while Eq. 5.8 represents the nearest neighbor. If $\vec{y}_{NN}(n)$ is not a false neighbor $\vec{y}(n)$, is truly a near neighbor of it, then this means that $\vec{y}_{NN}(n)$ is really neighbor to $\vec{y}(n)$ in physical meaning. The real attractors in nature are tightly packed in phase space and because of that, there can be many neighbors around the points in phase

space. By weeding out all of the false neighbors, we can identify the dimension d_e where the attractor becomes unfolded.

We can use a geometrical construction to do this [47]: If we have the false neighbor vector $\vec{y}_{NN}(n)$ coming from the projection from a higher dimension to the corresponding dimension d , we can lose the false neighbor to go out of the neighborhood of $\vec{y}(n)$ by going to a higher dimension $d + 1$.

While we go from dimension d to $d + 1$, we add additional components to both $\vec{y}(n)$ and $\vec{y}_{NN}(n)$; respectively, $s(n + d\tau)$ and $s_{NN}(n + d\tau)$. We can figure out which one of the neighbors is true and false by comparing the distances between the vectors $\vec{y}(n)$ and $\vec{y}_{NN}(n)$ in both dimension d and $d + 1$. If the corresponding distances are similar, then it means that the neighbor is true; if the distance we get for dimension d is smaller than the other, it means that the neighbor is false. Let's see the method analytically:

$$[R_d(n)]^2 = \sum_{m=1}^d [s(n + (m - 1)\tau) - s_{NN}(n + (m - 1)\tau)]^2, \quad (5.9)$$

where R_d is the Euclidian distance between the nearest neighbor points in dimension d . For the next dimension it becomes as follows:

$$[R_{d+1}(n)]^2 = \sum_{m=1}^{d+1} [s(n + (m - 1)\tau) - s_{NN}(n + (m - 1)\tau)]^2 \quad (5.10.a)$$

$$= [R_d(n)]^2 + |s(n + d\tau) - s_{NN}(n + d\tau)|^2 \quad (5.10.b)$$

Subtracting Eq. 5.9 from Eq. 5.10 and dividing by R_d gives the ratio of the distance between the neighbor points:

$$\sqrt{\frac{[R_{d+1}(n)]^2 - [R_d(n)]^2}{[R_d(n)]^2}} = \frac{|s(n + d\tau) - s_{NN}(n + d\tau)|^2}{R_d(n)} \quad (5.11)$$

The ratio in Eq. 5.11 can be used as a criterion. If the ratio is larger than some threshold, the neighbor is false.

5.4. FINDING THE LYAPUNOV EXPONENT

A way to see whether or not a system is chaotic is to look at the Lyapunov exponent. The Lyapunov exponent of a system is simply the averaged exponent of the divergence of exponentially diverging nearby trajectories of the system. A positive maximal Lyapunov exponent indicates that the system is chaotic.

If we want to find the maximal Lyapunov exponent of a time series, we can choose a point s_{n_0} whose neighbors are in the locality of ε . Then, we find the average of the distances of all neighbors to the reference part of the trajectory as a function of relative time. The logarithm of the average distance at time Δn gives an expansion rate over the time span Δn which includes all the fluctuations due to the projection and dynamics. Hence, we need to compute Eq. 5.12 to find the maximal Lyapunov exponent:

$$S(\Delta n) = \frac{1}{N} \sum_{n_0=1}^N \ln \left(\frac{1}{|U(s_{n_0})|} \sum_{s_n \in U(s_{n_0})} |s_{n_0+\Delta n} - s_{n+\Delta n}| \right) \quad (5.12)$$

s_{n_0} represents the embedding vectors, U is the neighborhood of s_{n_0} with diameter ε . We need to choose ε carefully to avoid missing information. It should be large enough to contain a sufficient number of neighbors to characterize a system and it should not be so large that missing of a small periodic component occurs. If there is a strict linear increase for some range on the graph of $S(\Delta n) - \Delta n$, the slope gives an estimation for the maximal Lyapunov exponent per time step.

5.5. HURST'S RESCALED RANGE ANALYSIS

In 1965, the British hydrologist Hurst introduced a method to obtain a measure of the variability of a time series in his work on the water storage of the Nile River [48]. The method provides an estimation of how variability of a time series changes with the length of the considered time period. The rescaled range (R/S) can be calculated simply by dividing the range of the values in a part of the considered time series by the standard deviation of the corresponding values. For instance, in Hurst's study, the calculation of the R/S proceeds as follows:

Hurst's problem was to find the capacity of a reservoir that is needed for it to release a volume of water as much as the mean inlet. It was wanted to build a reservoir which never overflows or becomes empty. First, the mean is calculated for the time series:

$$\langle X \rangle_n = \frac{1}{n} \sum_{i=1}^n X_i, \quad (5.13)$$

where X_i is the time series, or the amount of water flowing from a lake to the reservoir for a year; n is the number of the years. Secondly, the cumulative deviate series is calculated with a mean adjusted series:

$$Y(t, n) = \sum_{i=1}^n (X_i - \langle X \rangle_n) \quad (5.14)$$

The range series is

$$R(n) = \max(Y(t, n)) - \min(Y(t, n)) \quad (1 \leq t \leq n), \quad (5.15)$$

which gives the difference between the maximum and the minimum amount of water in the reservoir. If the capacity of the reservoir is greater than $R(n)$, it does not overflow or becomes empty for n years. On the other hand, the standard deviation series is given as

$$S(n) = \sqrt{\frac{1}{n} \sum_{i=1}^n (X_i - \langle X \rangle_n)^2}. \quad (5.16)$$

Finally, R/S is simply the ratio of $R(n)$ to $S(n)$. The Hurst exponent*, H , which is a measure of long-term memory of time series, is given as the asymptotic behavior of the R/S as a function of time span n :

$$\left\langle \frac{R(n)}{S(n)} \right\rangle = cn^H \quad (n \rightarrow \infty), \quad (5.17)$$

* The exponent was first called K by Hurst, but then was called H in the honor of Hurst by Mandelbrot (1983), and after him the exponent became famous for scaling analysis method [21].

where c is a constant. According to Hurst, lots of phenomena can be described successfully by this scaling relation [21].

In conclusion, it is a numerical approach to the predictability of a time series. If the Hurst exponent (H) is close to 0.5, the process is a random walk (Brownian motion). A Hurst exponent (H) in the range $0 < H < 0.5$ implies non-random behavior in the time series and the process is called as sub diffusion, and in the range $0.5 < H < 1$ implies a time series with long range continuous evolution and the process is called as super diffusion. Sub diffusion regimes can be seen in various areas and it is also observed in condensed matter systems commonly as in this present study or as in Refs. [49, 50].



6. CHAOS IN CONDENSED MATTER SYSTEMS: CURRENT THROUGH THIN FILMS

As stated before, real systems behave nonlinearly and we can often observe chaos in nature. Dielectrics are known as the structures that exhibit chaotic behavior. We investigated the behavior of the transient current through some sample thin films. The transient current through a sample of $As_2S_3(Ag)$ and $As_2Se_3(Al)$ glass substrate analyzed in a similar way as the work on polymers [51, 52].

6.1. EXPERIMENTAL SETUP AND THE MEASUREMENT

The specimens under investigation were prepared as sandwiched metal-glass-metal structures with the glass as the isolating layer. 300 nm thick aluminum electrodes were thermally evaporated at 10^{-6} mbar on microscope glass slides cleaned in a detergent solution. Subsequently, aluminum top contacts were evaporated. The I-V measurement was performed via a programmable picoammeter/voltage source (Keithley, model 487) and a temperature controller (Lake Shore, model 300). The picoammeter and the temperature controller were interfaced to a computer through an interface card that automated data taking, schematically presented in Figure 6.1. The picoammeter model 478 used is capable of reading currents in the range 10 fA to 2 mA. It also serves as a DC voltage supply in the range up to 500V.

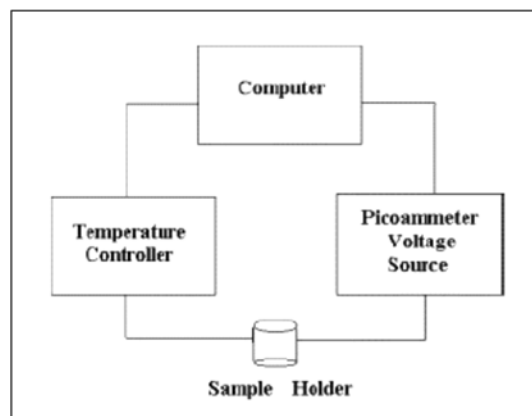


Figure 6.1. Schematic of the experimental setup.

The data of transient current against time for $As_2S_3(Ag)$ and $As_2Se_3(Al)$ are presented in Figures 6.2 and 6.3 respectively. Horizontal unit represents 30 ms. Examining the graphs, we find that there is an overall relaxation in $As_2Se_3(Al)$, but not in $As_2S_3(Ag)$. However, for both materials the data look more like the behavior of the transient current data for polymer thin films such as PMMA [52] or PEG-Si [51].

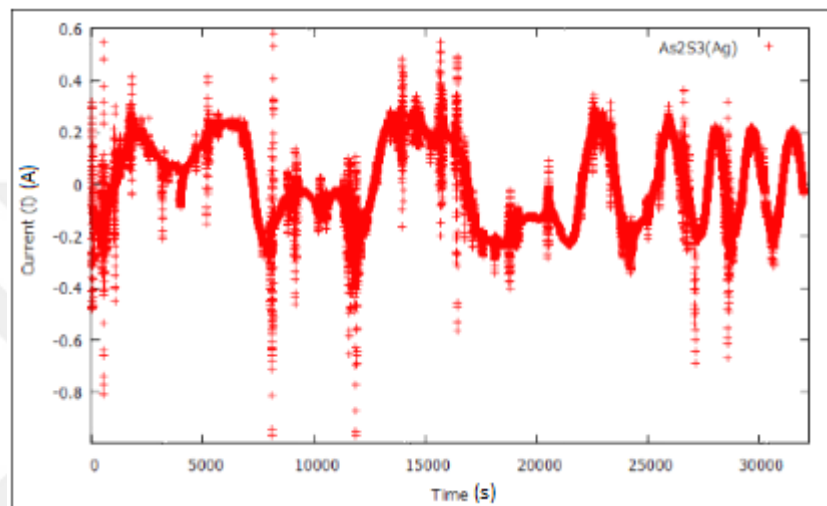


Figure 6.2. The data of $As_2S_3(Ag)$

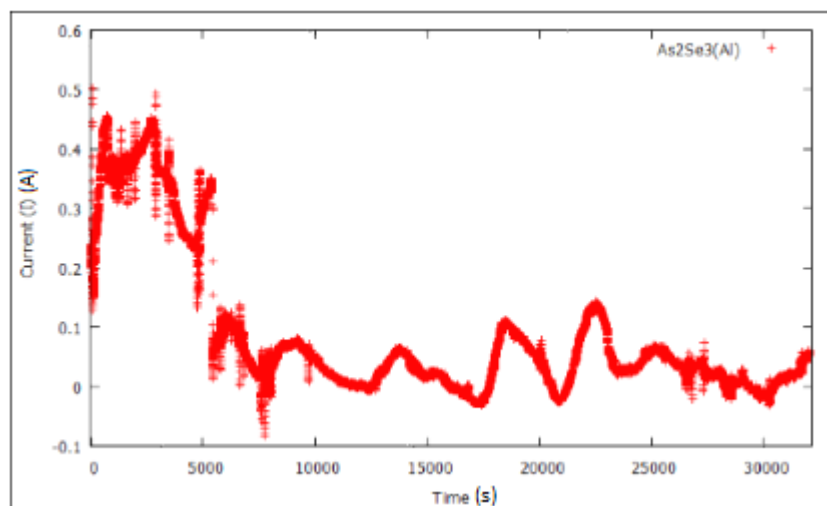


Figure 6.3. The data of $As_2Se_3(Al)$

6.2. THE ANALYSIS

We used TISEAN [54, 55] software package for time series analysis. We observe one dimensional signal in uniform time intervals, $x(0), x(T), \dots, x(nT)$. In fact, the signal $x(T)$ depends on an unknown number of parameters. To determine the number of parameters (dimensionality of the system), we find the meaningful time delay τ and the meaningful embedding dimension to construct time delay vectors. We find the embedding dimension by using the False Nearest Neighbors (FNN) method. We find the delay time by using Mutual Information (MUT) or correlation function (CORR). We calculate the auto correlation function which is the Fourier transform of the power spectrum and we present the results in Figure 6.4.

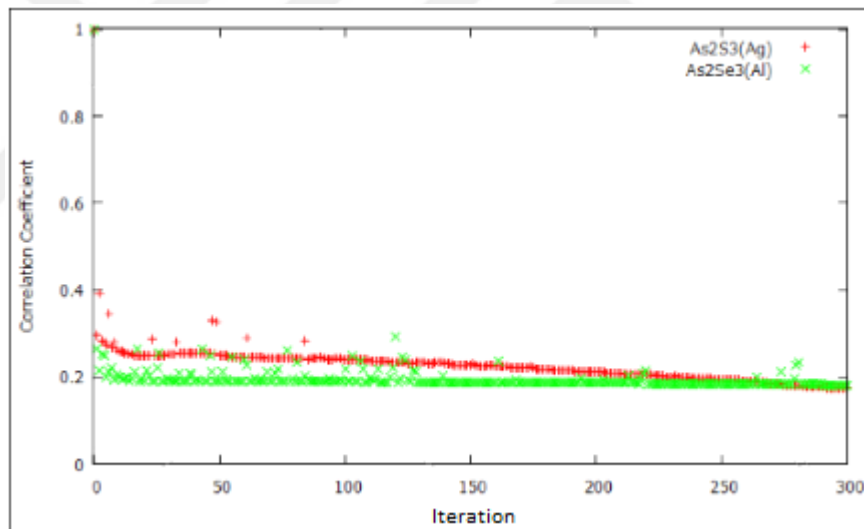


Figure 6.4. Correlation coefficient.

Another method for obtaining the delay time is to find the first minimum of the mutual information as presented in Figure 6.5. We wish to represent a random variable with actual probability distribution $p(x)$ with a code whose average length is $H(p)$. In practice, because of missing information or sampling, we may not know the actual distribution $p(x)$, so that we have to take the distribution to be $q(x)$. In such a situation, we may need a longer code to represent the random variable. This difference in length, $D(p(x)||q(x))$ is known as the relative entropy. The knowledge that one random variable includes about

another random variable is known as mutual information. We can only examine the information that we send to one channel in terms of information output from there. Let x and y be random variables with mutual distribution $p(x, y)$. If variables x and y have distributions $p(x)$ and $p(y)$, the mutual information is the entropy between the mutual distribution and product distribution. If it is chosen to be too small, $x(t)$ and $x(t + \tau)$ will be very close to each other and it will be difficult to distinguish them. If it is chosen too large, $x(t)$ and $x(t + \tau)$ coordinates will be too far apart, will behave independently and cause loss of information.

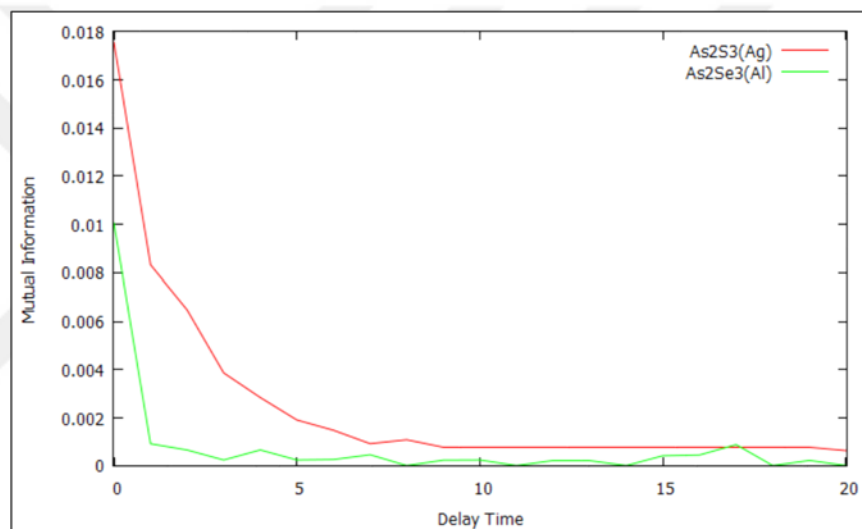


Figure 6.5. Mutual information.

False nearest neighbors graph (FNN) presented in Figure 6.6 is useful for determining the minimal embedding dimension. The purpose is to find points near each other in the embedded space. If the embedding dimension is too small, points that are close in embedded space will appear as false neighbors. If the embedding dimension is too large, we lose statistics and information. By expressing the distance in $(d + 1)$ dimensions in terms of the distance in d dimensions, we can calculate the number of neighbors in d and $(d + 1)$ dimensions, R_{d+1}/R_d . If this ratio is above a critical value, we have false nearest neighbors.

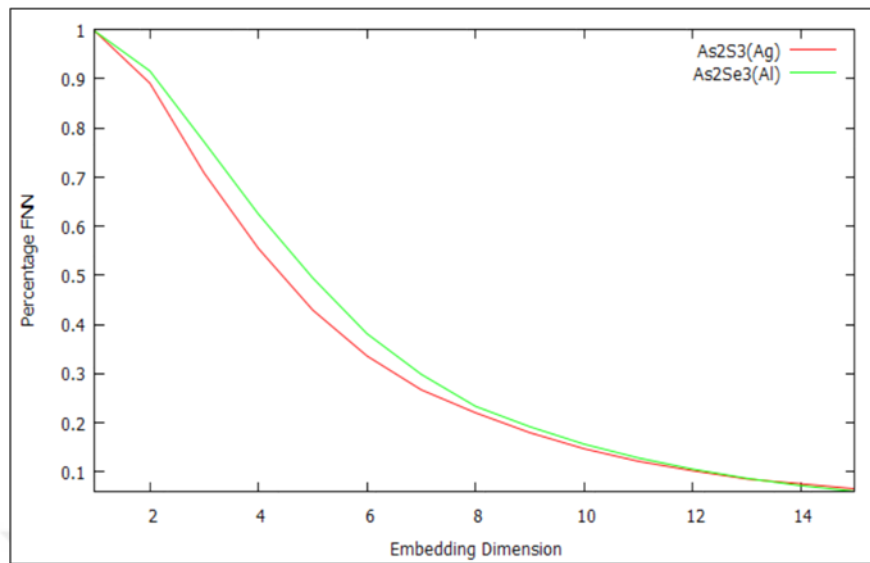


Figure 6.6. False nearest neighbors.

The largest Lyapunov exponent presented in Figure 6.7 is usually used as an indicator of chaos. This is obtained by calculating the quantity in Eq. 5.12.

In Eq. 5.12, s_{n_0} is our reference point, U is a hypersphere of distance ε to this point. If ε is too small, we cannot find a sufficient number of points, if it is too large, a periodic component may be missed. For a few ε values, calculating the number of points in the hypersphere $S(\Delta n)$, plotting it against Δn gives the largest Lyapunov Exponent. A positive slope implies a positive Lyapunov Exponent.

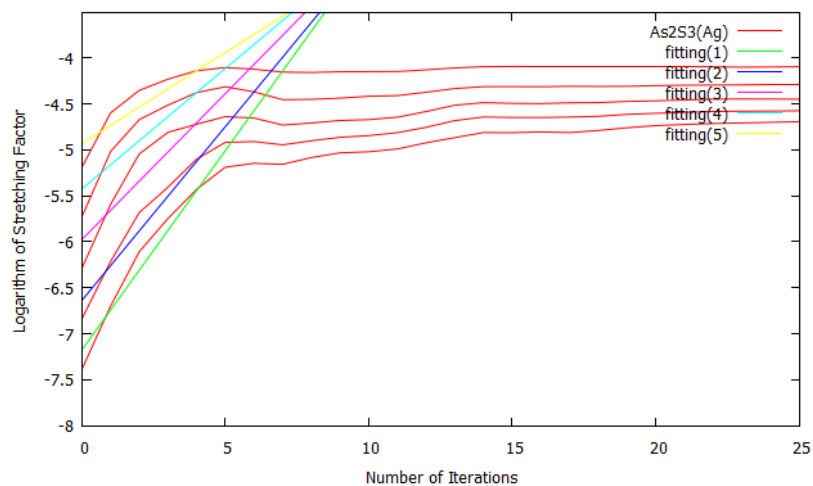


Figure 6.7. Largest Lyapunov Exponents with every line for $As_2S_3(Ag)$.

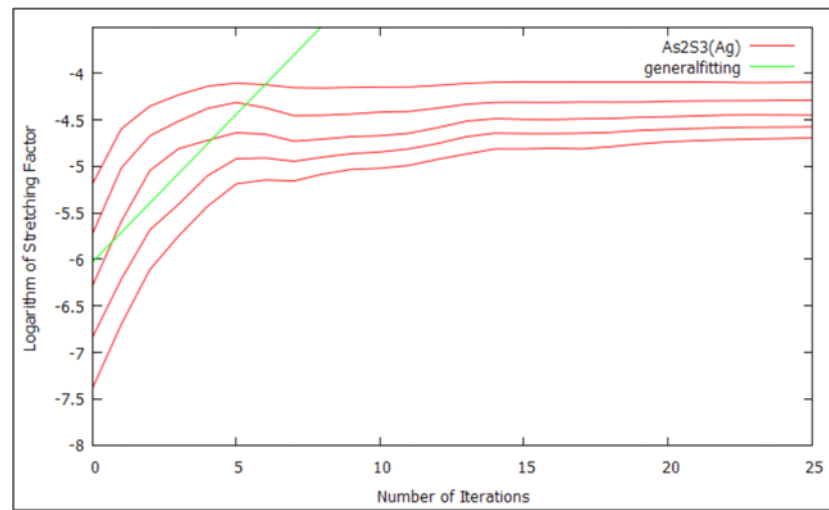


Figure 6.8. Largest Lyapunov exponent with average line for $As_2S_3(Ag)$.

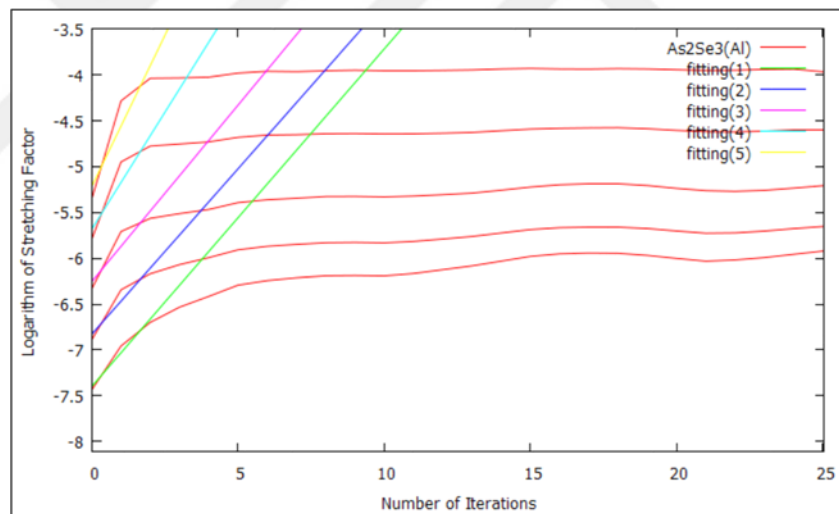


Figure 6.9. Largest Lyapunov Exponents with every line for $As_2Se_3(Al)$.

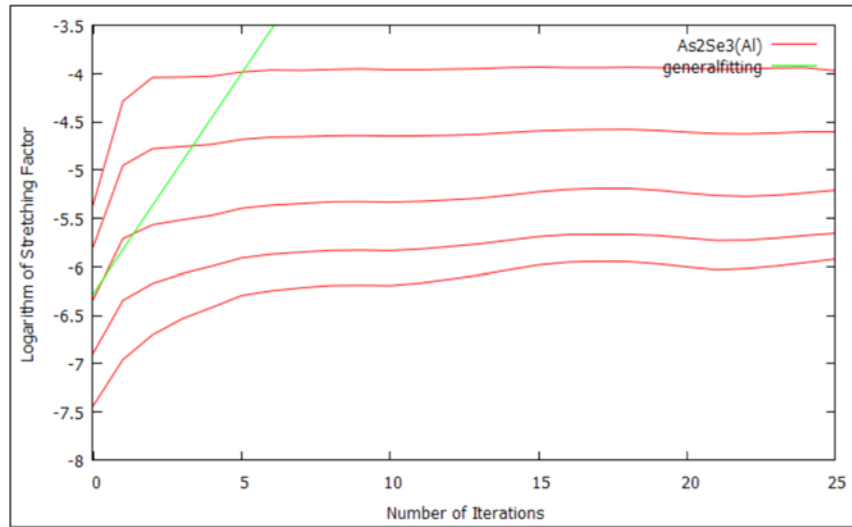


Figure 6.10. Largest Lyapunov exponent with average line for $As_2Se_3(Al)$.

Table 6.1. Lyapunov Exponents extracted from the data of $As_2S_3(Ag)$ and $As_2Se_3(Al)$.

Thin Films	Lyapunov Exponent (slope)
$As_2S_3(Ag)$	0.317
$As_2Se_3(Al)$	0.456

We also find the Hurst exponent by using the standard approach as described in section 5.5, and as presented in Figure 6.11.

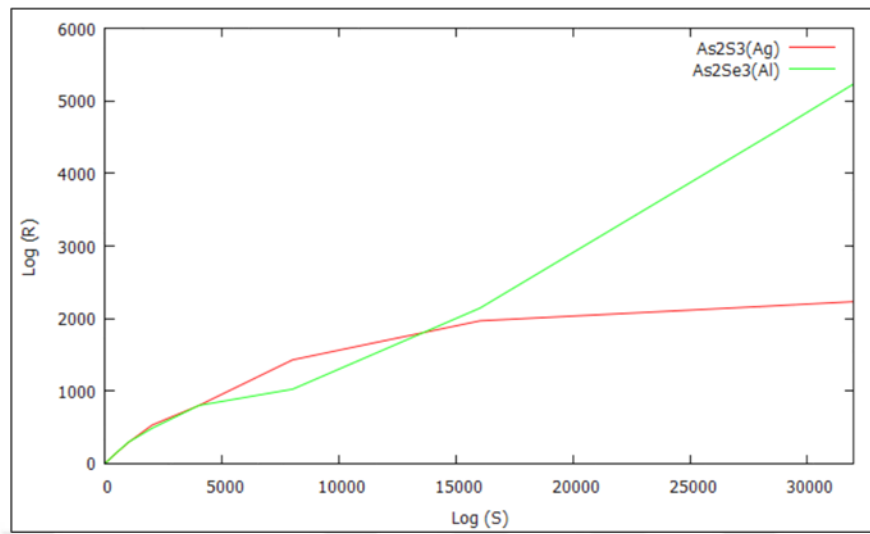


Figure 6.11. Hurst Analysis.

7. *q*-GAUSSIAN ANALYSIS OF THE ELECTRONIC BEHAVIOR IN $As_2S_3(AG)$ AND $As_2Se_3(AL)$ THIN FILMS

In the context of *q*-statistics, *q*-Gaussian analysis can be used to interpret systems which show weak chaotic behavior, that is, the systems which have Lyapunov exponents near zero [56]. Our data of the transient current through a sample of $As_2S_3(AG)$ and $As_2Se_3(AL)$ glass substrates were examined with *q*-Gaussian analysis in a similar way as the work on polymers [57]. We aimed to see the applicability of *q*-statistics to transient current in thin films and to observe if the results of the *q*-Gaussian analysis show consistency with the results summarized in chapter 6. Since *q*-statistics is an analytical tool which is independent from those of chaos theory; the previous results (Chp. 6) can support or deny the present results of *q*-Gaussian analysis.

7.1. THE ANALYSIS

It is not possible to analyze data which show weak chaoticity with classical statistical mechanical tools. However, nonextensive statistical mechanics [58] is found to be useful for such analysis. $As_2S_3(AG)$ and $As_2Se_3(AL)$ data can be fitted by a *q*-Gaussian curve, much better than it would be for a normal Gaussian. Rewriting Eq. 4.22 gives

$$p(x) = A[1 - (1 - q)x^2/B]^{1/(1-q)}, \quad (7.1)$$

where *A* and *B* are constants. We calculated the difference of each successive current value $I(t)$ over the whole measurement span:

$$I(t) = i(t + 1) - i(t) \quad (7.2)$$

Then, $I(t)$ was normalized by subtracting its mean value over time and dividing the result by the standard deviation:

$$\frac{I(t) - \langle I(t) \rangle}{\sigma(I(t))} \quad (7.3)$$

The histograms of the data were computed and the distributions were plotted against the normalized $I(t)$. The resulting distributions were fitted to a q -Gaussian curve by picking suitable A and B parameters and also finding a suitable value for q . The probability density functions (PDF) against normalized $I(t)$ can be seen in figures 7.1 and 7.2.

In figures 7.1 and 7.2, the PDFs of the current magnitude differences (Eq. 7.2) for the transient current through thin $As_2S_3(Ag)$ and $As_2Se_3(Al)$ films. The curves fitted to a typical q -Gaussian with exponents $q = 2.0$ and $q = 2.4$ respectively. The values we obtained from the fits can be seen in Table 7.1.

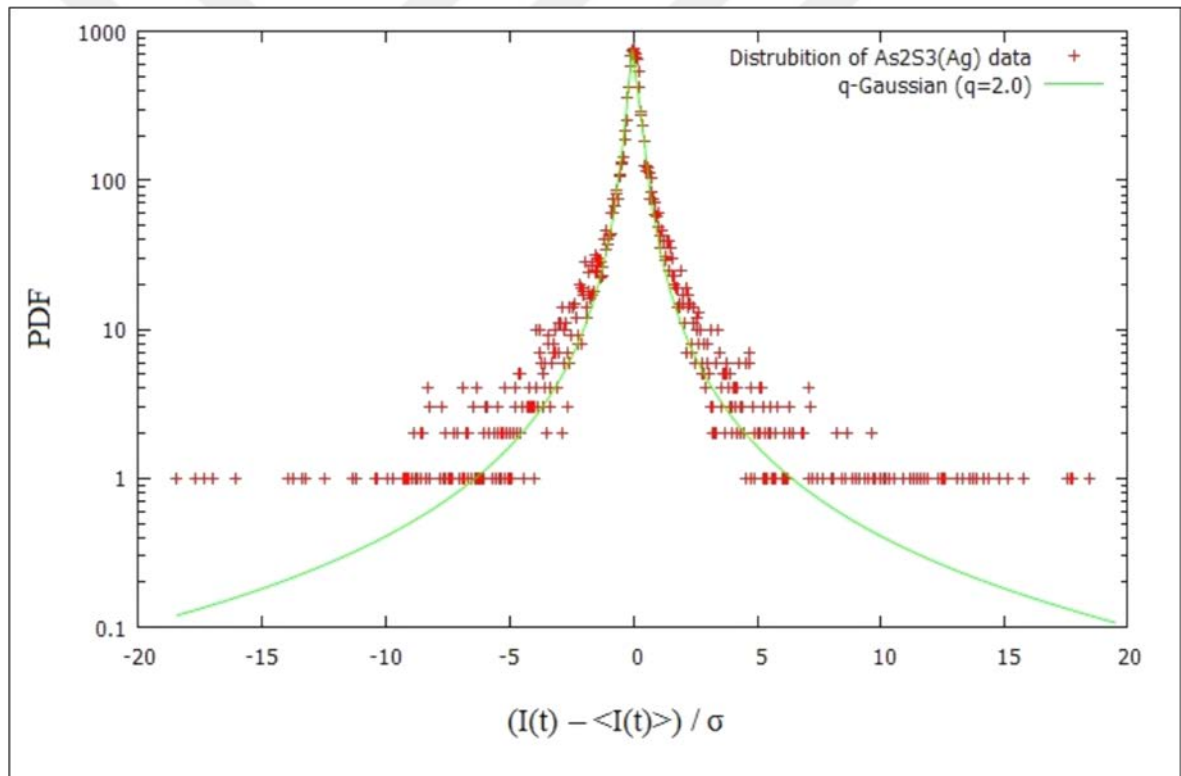


Figure 7.1. PDF of the current magnitude differences for the transient current through thin $As_2S_3(Ag)$. The curve has been fitted with a q -Gaussian (green line) with an exponent $q = 2.0$.

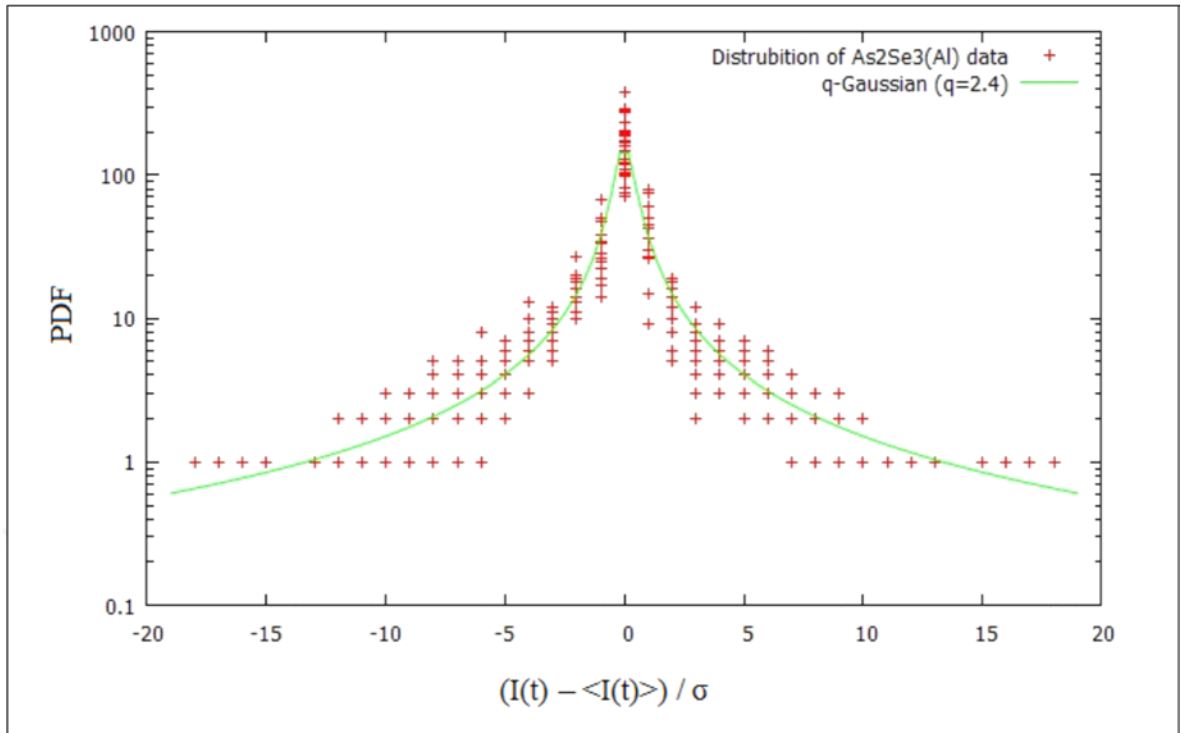


Figure 7.2. PDF of the current magnitude differences for the transient current through thin $As_2Se_3(Al)$. The curve has been fitted with a q -Gaussian (green line) with an exponent $q = 2.4$.

Table 7.1. A , B and q parameter values of the fitted q -Gaussian function.

	A	$1/B$	q
$As_2S_3(Ag)$	796.9	19.5	2.0
$As_2Se_3(Al)$	167.8	5.2	2.4

8. CONCLUSION

The complex structure of chalcogenites suggests many degrees of freedom and a multi-fractal structure. The transient current through the samples of $As_2S_3(Ag)$ and $As_2Se_3(Al)$ glass substrates has been analyzed in order to study possible chaotic behavior similar to that in the work on polymers [51, 52] and [57].

The conductivity mechanism measured by the time dependent behavior of transient current was analyzed by nonlinear considerations such as time series analysis, maximal Lyapunov exponent, Hurst (R/S) analysis. Intermediate dimensional chaos with positive maximal Lyapunov exponents was observed. The behaviors of the system with possibly two different regions, one with short range and another with long range correlation were seen by comparing the correlation coefficient and mutual information.

Since the maximal Lyapunov exponents are small, the thin films we used seemed like exhibiting weak chaos. Nonextensive statistics or q -statistics are suitable for analysis of data exhibiting weak chaos. To get more information about the behavior of transient current through the corresponding samples, we have analyzed our data by using q -statistics. We observed a behavior different from a Gaussian one. The curves are peaked and they have long tails. Thus, we obtained non-Gaussian probability density functions. q exponents are greater than 1 as we expected, where at $q = 1$ the q -Gaussian recovers the normal Gaussian. All results imply that there is a chaotic behavior. The complex structure of the sample thin films may support a number of conduction mechanisms that are acting simultaneously and affecting each other so that the current fluctuations bring forth a q -Gaussian shape of the PDFs. In conclusion for the latter part, we saw the applicability of q -statistics to transient current in thin films in our study and we observed how the results of q -Gaussian analysis show consistency with the first results. Moreover, by the two analysis we saw that the transient current behavior of $As_2S_3(Ag)$ and $As_2Se_3(Al)$ films manifest chaotic behavior which is not strong. As suggested by studies of other amorphous materials with irregular behavior, the use of nonlinear methods for analyzing the conductivity mechanisms in such materials seems crucial in modeling and show that the behaviors are comparable.

REFERENCES

1. K. Popper. *The Logic of Scientific Discovery*, Routledge, London, 2002.
2. Hesiod. *Hesiod's Theogony*, Focus Information Group, Inc., Newburyport MA, 1987.
3. E. N. Lorenz. Deterministic nonperiodic flow. *Journal of the Atmospheric Sciences*, 20: 130, 1963.
4. J. Gleick. *Chaos*, Viking Penguin, New York, 1987.
5. S. H. Strogatz. *Nonlinear Dynamics And Chaos With Applications to Physics, Biology, Chemistry, and Engineering*, Perseus Books Publishing, 1994.
6. Wolfram Demonstration Project, <http://demonstrations.wolfram.com> [retrived 11 November 2014].
7. D. Ruelle, and F. Takens. On the nature of turbulence. *Communications in Mathematical Physics*, 20: 167, 1971.
8. U. Feudel, S. Kuznetsov, and A. Pikovsky. *Strange Nonchaotic Attractors: Dynamics between Order and Chaos in Quasiperiodically Forced Systems*, World Scientific Publishing Co. Pte. Ltd., Singapore, 2006.
9. Logical Tightrope: Physics with a Spin, "Edward Lorenz's Strange Attraction", <http://logicaltightrope.com/2013/08/29/edward-lorenzs-strange-attraction/> [retrived 8 December 2014].
10. S. Smale. Differentiable dynamical systems. *Bulletin of the American Mathematical Society*, 73: 747-817, 1967.

11. N. Kaldor. A Classificatory Note on the Determination of Equilibrium. *Review of Economic Studies*, vol 1: 122-136, 1934.
12. R. M. May. Simple mathematical models with very complicated dynamics. *Nature*, 261: 459, 1976.
13. B. Mandelbrot. How Long is the Coast of Britain? Statistical Self-Similarity and Fractional Dimension. *Science*, 156(3775): 636–638, 1967.
14. C. A. Pickover. *The Math Book: From Pythagoras to the 57th Dimension, 250 Milestones in the History of Mathematics*, Sterling Publishing Company, 2009.
15. H. J. S. Smith. *On the integration of discontinuous functions. Proceedings of the London Mathematical Society*, Series 1, vol. 6, 140-153, 1874.
16. H.-O. Peitgen, H. Jürgens, and D. Saupe. *Chaos and Fractals: New Frontiers of Science*, 2nd ed., Springer Verlag, New York, 2004.
17. M. F. Barnsley. *Fractals Everywhere*, Morgan Kaufmann, San Francisco, 1993.
18. A. Fick. Über Diffusion. *Poggendorf's Annalen der Physik und Chemie*, 94: 59-86, 1855. In English: *Philosophical Magazine*, Series 4, vol. 10, 30-39, 1855.
19. F. M. H. Villars, and G. B. Benedek. *Physics with Illustrative Examples from Medicine and Biology*, Addison-Wesley Publishing, Massachusetts, 1974.
20. R. Brown. A brief account of microscopical observations made in the months of June, July and August, 1827, on the particles contained in the pollen of plants; and on the general existence of active molecules in organic and inorganic bodies. *Philosophical Magazine*, 4: 161-173, 1828.
21. N. Scafetta. *Fractal and Diffusion Entropy Analysis of Time Series*, VDM Verlag Dr. Müller, Saarbrücken, 2010.

22. C. Tsallis. Possible generalization of Boltzmann-Gibbs statistics. *Journal of Statistical Physics*, 52, 1-2: 479-487, 1988.
23. C. Tsallis. *Introduction to Nonextensive Statistical Mechanics: Approaching a Complex World*, Springer, New York, 2009.
24. S. Abe, and Y. Okamoto. *Nonextensive Statistical Mechanics and Its Applications*, Springer, Berlin, 2001.
25. M. Gell-Mann, and C. Tsallis. *Nonextensive Entropy: Interdisciplinary Applications*, Oxford University Press, New York, 2004.
26. L. Boltzmann. *Weitere Studien über das Warmegleichgewicht unter Gas molekulen* [Further Studies on Thermal Equilibrium Between Gas Molecules], Wien, Ber.,66: 275, 1872.
27. L. Boltzmann. Über die Beziehung eines allgemeine mechanischen Satzes zum zweiten Hauptsatz der Warmetheorie. *Sitzungsberichte, K. Akademie der Wissenschaften in Wien, Math.-Naturwissenschaften* 75, 67, 1877.
28. L. Boltzmann. On the Relation of a General Mechanical Theorem to the Second Law of Thermodynamics. In: S. Brush, *Kinetic Theory*, vol. 2: *Irreversible Processes*, 188, Pergamon Press, Oxford, 1966.
29. J.W. Gibbs. *Elementary Principles in Statistical Mechanics – Developed with Especial Reference to the Rational Foundation of Thermodynamics*, C. Scribner's Sons, New York, 1902.
30. O. Penrose. *Foundations of Statistical Mechanics: A Deductive Treatment*, Pergamon Press, Oxford, 1970.

31. C. Tsallis. What are the numbers that experiments provide? *Quimica Nova*, 17: 468, 1994.
32. S. Picoli, R. S. Mendes, and L. C. Malacarne. q-exponential, Weibull and q-Weibull distributions: an empirical analysis. *Physica A: Statistical Mechanics and its Applications*, 324: 678, 2003.
33. S. Picoli Jr., R. S. Mendes, L. C. Malacarne, and R. P. B. Santos. q-distributions in complex systems: a brief review. *Brazilian Journal of Physics*, 39(2A): 468-474, 2009.
34. N. Gradojevic, and R. Gencay. Overnight Interest Rates and Aggregate Market Expectations. *Economics Letters*, 100(1): 27–30, 2008.
35. M. Kozaki, and A. H. Sato. Application of the Beck model to stock markets: Value-at-Risk and portfolio risk assessment. *Physica A: Statistical Mechanics and its Applications*, 387: 1225-1246, 2008.
36. D. A. Moreira, E. L. Albuquerque, L. R. da Silva, and D. S. Galvao. Low temperature specific heat spectra considering nonextensive long-range correlated quasiperiodic DNA molecules. *Physica A: Statistical Mechanics and its Applications*, 387: 5477-5421, 2008.
37. M.Bozejko, B. Kümmerer, and R. Speicher. q-Gaussian Processes: Non-commutative and Classical Aspects. *Communications in Mathematical Physics*, 185: 129-154, 1997.
38. E. Yee, P. R. Kosteniuk, G. M. Chandler, C. A. Biltoft, and J. F. Bowers. Recurrence statistics of concentration fluctuations in plumes within a near-neutral atmospheric surface layer. *Boundary-Layer Meteorology*, 66: 127-153, 1993.
39. F. Caruso, A. Pluchino, V. Latora, S. Vinciguerra, and A. Rapisarda. Analysis of self-organized criticality in the Olami-Feder-Christensen model and in real earthquakes. *Physical Review E*, 75: 055101, 2007.

40. F. C. Moon. *Chaotic and Fractal Dynamics: An Introduction for Applied Scientists and Engineers*, John Wiley and Sons, New York, 1992.
41. J. M. T. Thompson, and H. B. Stewart. *Nonlinear Dynamics and Chaos*, John Wiley and Sons, Chichester, 1986.
42. J. Guckenheimer, and P. Holmes. *Nonlinear Oscillations, Dynamical Systems, and Bifurcations of Vector Fields*, Springer, New York, 1983.
43. H. D. I. Abarbanel. *Analysis of Observed Chaotic Data*, Springer Verlag, New York, 1996.
44. F. Takens. Detecting strange attractors in turbulence. In: D. A. Rand, and L.-S. Young, *Dynamical Systems and Turbulence, Lecture Notes in Mathematics*, vol. 898, Springer-Verlag, Berlin, 1981.
45. F. Takens. On the numerical determination of the dimension of an attractor. In: B.L.J. Braaksma, H.W. Broer, and F. Takens, editors, *Dynamical Systems and Bifurcations, Lecture Notes in Mathematics*, vol. 1125, Springer-Verlag, Berlin, 1985.
46. R. G. Gallager. *Information Theory and Reliable Communication*, John Wiley and Sons, New York, 1968.
47. M. B. Kennel, R. Brown, and H. D. I. Abarbanel. Determining embedding dimension for phase-space reconstruction using a geometrical construction. *Physical Review A*, 45: 3403-3411, 1992.
48. H. E. Hurst, R. P. Black, and Y. M. Simaika. *Long-term storage: an experimental study*, London, Constable, 1965.
49. G. Pfister, and H. Scher. Time-dependent electrical transport in amorphous solids: As_2Se_3 . *Physical Review B*, 15: 2062-2083, 1977.

50. G. Pfister, and H. Scher. Dispersive (non-Gaussian) transient transport in disordered solids. *Advances in Physics*, 27: 747-798, 1978.
51. O. Ö. Aybar, A. Hacinliyan, Y. Skarlatos, G. Sahin, and K. Atak. Possible Stretched Exponential Parametrization for Humidity Absorption in Polymers. *European Physical Journal E*, 28: 369-376, 2009.
52. O. Ö. Aybar, A. Hacinliyan, Y. Skarlatos, G. Şahin, and K. Atak. Chaoticity analysis of the current through pure, hydrogenated and hydrophobically modified PEG-Si thin films under varying relative humidity. *Central European Journal of Physics*, 7: 568-574, 2009.
53. Y. Skarlatos, G. Şahin, and G. Akın. Signals of Chaotic Behavior in PMMA. *Chaos Solitons and Fractals*, 17: 575-583, 2003.
54. R. Hegger, H. Kantz, and T. Schreiber. Practical implementation of nonlinear time series methods: The TISEAN package. *Chaos*, 94: 413, 1999.
55. H. Kantz, and T. Schreiber. *Nonlinear Time Series Analysis*, Cambridge University Press, Cambridge, 1997.
56. G. Miritello, A. Pluchino, and A. Rapisarda. Central Limit behavior in the Kuramoto model at the 'Edge of Chaos'. *Journal of Physics A*, 388: 4818-4826, 2009.
57. G. C. Yalçın, Y. Skarlatos, and K. G. Akdeniz. q-Gaussian Analysis in Complex Polymers. In: *Proceedings of the Conference in Honor of Murray Gell-Mann's 80th Birthday Quantum Mechanics, Elementary Particles, Quantum Cosmology and Complexity*, World Scientific Publishing, Singapore, 669-672, ISBN: 978-981-4335-60-7, 2010.
58. C. Tsallis, M. Gell-Mann, and Y. Sato. Extensivity and Entropy Production. *Europhysics News*, 36: 6, November-December 2005.